d Collection

Thesis for the Degree of Master of Science

Towards Universal Haptic Library–Library-Based Haptic Texture Assignment Using Image Texture

Waseem Hassan

Department of Computer Science and Engineering

Graduate School

Kyung Hee University

Seoul, Korea

August, 2016

Towards Universal Haptic Library–
Library-Based Haptic Texture Assignment
Using Image Texture

Waseem Hassan

Department of Computer Science and Engineering
Graduate School
Kyung Hee University
Seoul, Korea

August, 2016

Towards Universal Haptic Library–
Library-Based Haptic Texture Assignment
Using Image Texture

by

Waseem Hassan

Supervised by

Prof. Seokhee Jeon, Ph.D.

Submitted to the Department of Computer
Science and Engineering
and the Graduate School of Kyung Hee University
in partial fulfillment of the requirements
for the degree of Master of Science

Dissertation Committee:

Prof. Seungkyu Lee, Ph.D. ....

Prof. Oksam Chae, Ph.D. ....

Prof. Seokhee Jeon, Ph.D. ....

Abstract

The main focus of this research was to build a universal haptic texture models library and to design an automatic haptic model assignment algorithm which is used to assign haptic models to any given texture surface based on image features. Evidence of a relation between perceptual haptic texture and image features is provided and this relationship is used in the automatic assignment of haptic texture models. Haptic texture perceptual space and image feature space are established and the correlation between the spaces was found. The correlation from these two spaces was used to train a multi-class support vector machine with a radial basis function kernel resulting in a universal haptic texture library comprising of 84 real life texture surfaces. The perceptual space was classified into perceptually similar clusters using K-means. Haptic texture models were assigned to new surfaces in a two step process; classification into a perceptually similar group using the trained multi-class support vector machine, and finding a unique match from within the group using binarized statistical image features. The system was evaluated using 21 new real life texture surfaces and an accuracy of 71.4% was achieved in assigning haptic models to these surfaces.

Acknowledgment

I would like to thank my supervisor Dr. Seokhee Jeon for guiding me through out my tenure as a master's student. His invaluable advice, suggestions, and guidance has helped me in improving my knowledge and skill set. He has put in a lot of effort in shaping me into a better researcher. I am truly grateful for all his support. I would also like to extend my gratitude towards my lab mate Arsen Abdulali. He was a constant source of motivation and encouragement for me. His insightful comments and ideas went a long way in improving my research.

I would like to thank my family members for their constant support. I dedicate all my success to them because it was only possible with their constant support and countless prayers.
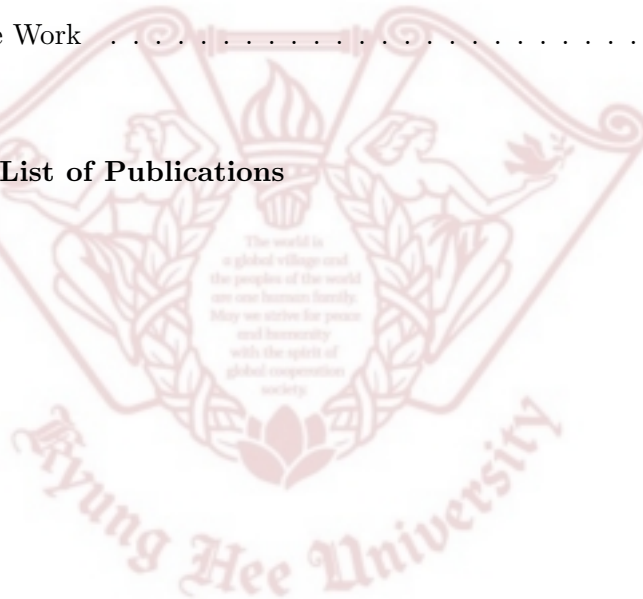
Waseem Hassan

August, 2016

Table of Contents

List of Figures

List of Tables

x

Chapter 1

Introduction

1.1 Haptic Texture Modeling

In recent decades the field of virtual reality (VR) has improved by leaps
and bounds. It has found applications across a multitude of research and
commercial areas [1–9]. In a VR system, the actions and behavior of a
user are closely monitored and the environment is altered accordingly. The
response of the virtual environment to a user's actions is in the form of
a feedback. This feedback can be visual, auditory, or any other modality.
The aim of such virtual reality environments is to keep the user interacted
and indulged in the created environment, ideally to such an extent that
the user cannot distinguish the virtual environment from a real one. This
interactiveness, in more technical terms, is called as the immersiveness or
realism of the virtual reality system or environment. Until recent times,
VR systems used to incorporate most of the sensory modalities with the
exception of the haptic modality. But recent VR systems, with the addition
of haptic content, has a vastly improved immersiveness and realism [10–13].
However, the provision of haptic feedback is not as straightforward as other
modalities nor it is as developed as others.

One of the most stringent bottlenecks in haptics technology for VR sys-
tems is the difficulty in providing haptic models. The provision of haptic
feedback for VR environments basically requires two things; a geometric

model of the environment, and the haptic property models which are associated with the geometry of the environment [14]. The provision of a geometric model for the environment is a relatively easy task since a single model is usually shared, and various computer graphics tools and algorithms are readily available for creating a geometric model. However, haptic property models e.g., friction, stiffness, surface texture, etc. are much harder to obtain. Mostly there are two methods for obtaining haptic property models. The first one is concerned with the manual tuning of parametric models [15–17]. While the other method, as carried out in [18–20] ,involves training of non-parametric interpolation methods. In order to provide a virtual haptic feedback for a given object, a object needs to be interacted with using a sophisticated sensing hardware or should be felt by the designers to judge its properties for manual tuning of parameters.

Another hindrance in the haptic modeling process is the association of appropriate haptic properties with the corresponding geometric model. Currently, this association is mostly carried out manually in the code for rendering haptic feedback. However, initial efforts have been made for providing a tool for handling haptic properites intuitively [21, 22].

1.2   Perceptual Differences Between Bare Handed and Tool Based Interaction

It is not uncommon in our everyday life to find situations where the use of a finger or hand for interaction is not possible. For example, when we encounter a seemingly hot surface or if we have to write on a piece of paper. In such situations, the human finger or hand is substituted by a tool. Although, we are not in direct contact with the desired surface, we receive a rich haptic feedback through the tool [23].

Various studies have focused on the haptic perceptions of textures using either bare hand [24–26] or a tool [27–29]. A limited number of studies have taken up these two modes of interaction for comparison [30, 31].

Furthermore, most of the haptic rendering environments are tool based, while in our daily life we usually use our bare hands for interaction. Thus, it is of utmost importance to find out the underlying perceptual differences in the two modes of interaction. Such a study will help in improving the realism of haptic rendering environments by covering the gap between bare handed and tool based perception and as a result these environments can be molded towards providing a perceptually more realistic feedback.

1.3   Research Goal

The main aim behind this study is to provide a 'Universal Haptic Texture Models Library' where different haptic models, describing the haptic properties of a wide range of haptic surfaces, are stored. Additionally, our aim is to develop a system that uses the library to automatically assign haptic property models to the environment with minimum overload. Such a system would radically decrease the time and efforts required for extensive modeling of the haptic environment.

In an effort to achieve these goals, the current study provides an initial attempt towards image texture based automatic assignment of haptic models. It is a well known fact that image texture bears correlation with haptic texture, as shown in [32–34]. Furthermore, haptic texture of surface can be judged from the micro geometry of the surface, and this micro geometry of the surface can be readily captured in an image. Thus, in the current study, the perception aspects of images are used in automatic assignment of haptic texture models. The overall procedure of achieving these goals can

be defined in four major steps.

1 - Capture the haptic texture properties of real life surfaces, where the surfaces should cover a wide range of daily life haptic interactions. This can be achieved by conducting a user study to establish a perceptual space where the given surfaces are represented based on their perceptual haptic texture characteristics.

2 - Acquisition of a wide range of visual texture characteristics from the all the texture surfaces by extracting multiple image features.

3 - Determining a relationship between the haptic texture properties (perceptual space), i.e., step 1, and the visual texture properties (image features), i.e., step 2. As a result, establishing a library where the haptic texture models are stored along with the associated image features.

4 - Automatic assignment of haptic texture models to newly encountered - outside library - texture surfaces based on their image features using the library established in step 3.

1.4 Contributions

The main contributions of the current study are listed below:

- In the current study we used 84 real life texture surfaces for establishing the perceptual space and extraction of image features. All the surfaces were collected from daily life objects and the use of artificial or trivial surfaces was avoided. The use of such a dynamic range of texture surfaces is very rare in the field of haptics and perception.

- A relationship between haptic texture properties and image features was established.

- A universal haptic texture models library was established where haptic models were stored along with the corresponding image features.

- An automatic haptic models assignment algorithm was developed for assigning haptic models to arbitrary real life texture surfaces based on their image features.

- Differences between tool based and bare handed interaction were evaluated in the perceptual space using multidimensional analysis.

1.5   Organization

Various related works and the techniques used in this study are detailed in Chapter 2. The texture surfaces dataset used in the current research is described in Chapter 3. The building of a perceptual space from the haptic properties of the texture surfaces is explained in Chapter 4. In Chapter 5, the image feature extraction process is highlighted along with the image feature selection process. The automatic assignment of haptic texture models to various surfaces as well as the establishment of the universal haptic library is presented in Chapter 6. The evaluation process for checking the accuracy of the proposed algorithm is provided in Chapter 7. The effect of using a bare hand as compared to a tool for interaction is explained in Chapter 8. A brief conclusion and possible future works are discussed in Chapter 10.

Chapter 2

Related Works

One of the first attempt of making haptic models library was made in [35] where they established 100 different texture models for haptic rendering. Although this library might cover a large range of haptic interaction, but its has some fundamental drawbacks. First, there is no way to automatically assign a haptic model to new surfaces. In order to include a new texture model, the whole modeling process using data-driven haptic modeling has to be repeated. Second, selecting a perceptually similar model, from within the library, for a surface can be a cumbersome task as one has to manually search through the library for a close match. In order to overcome these drawbacks, the approach followed in the current study is to automate model assignment process. For this purpose a relationship between the visual and haptic characteristics of texture surfaces is established.

This chapter will describe the efforts made by researchers in building haptic texture perceptual spaces. The methods used for conducting the experiments for building perceptual spaces will also be touched upon. Afterwards, the various previous attempts at using visual information for identifying or classifying surface textures will be highlighted.

2.1 Establishing Haptic Texture Perceptual Space

Discovering the perceptual properties of textures surfaces has been the focus of various studies, mainly, neurophysiological and psychophysical. The researches related to perception of haptic properties have been summarized in various review papers [36–38]. A more recent study provides a taxonomy and detailed study of the haptic perceptual properties [26]. This study suggested that there are mainly five dimensions associated with perception of texture: hard, warm, friction, micro-roughness, and macro-roughness.

The number of dimensions in a perceptual space are highly dependent on the number and variety of texture surfaces used in the study. For example, [39] used only one kind of material, i.e., 40 fabrics. In [40], the authors again used 26 fabrics. Similarly, in [41] Lyne et al. used 8 tissues and paper towels. Although, these were very confined studies with a controlled group of textures, but could only discover two dimensions due to the limited range of the stimuli.

Hollins et al. in [42] used 17 different kinds of materials, Ballesteros et al. in [43] used 20 materials of varying nature , in [30] the authors used 16 materials. Due to the variety of surfaces used in these studies, three different dimensions were unearthed.

While, a unique study where the authors used 124 materials ranging from every aspect of haptic interaction, could find four dimensions in their perceptual space [44].

The psychophysical experiments conducted for building the perceptual spaces can be categorized into three basic categories [26]. The semantic differential(SD) [45] method where participants judge the textures on a scale of adjectives. On both ends of the scale are adjectives with opposite meaning. All the surfaces are evaluated separately. The advantage of such methods

is the use of adjectives, which can portray more meaning than mere numbers. But if a particular adjective is missing from the scale, the perceptual property associated with that adjective can also remain unextracted. This method is used in [46, 47].

The second type of method is the Estimation Method where human subjects are asked to rate the similarity between two given surfaces. However, since a participant has to rate every surface against every other surface in the study, the number of total comparisons increase exponentially with increase in the number of surfaces.

The third method is the clustering or classification method where participants are asked to classify perceptually similar surfaces into groups [42, 43]. This method is significantly fast as compared to other methods and therefore allows the use of a large number of surfaces to be compared. However, this method assumes that the surfaces within one group have no perceptual dissimilarity. However, recently in [48] the authors have shown that a cluster sorting experiment can successfully are reasonably accurately capture the minor dissimilarity details across surfaces.

Statistical methods are used to visualize the data from the perception analysis of different textures. The most famous and common statistical method is the Multi Dimensional Scaling (MDS) analysis. An introduction to MDS is provided in [49]. The perceptual spaces established as a result of MDS shows different texture surfaces as points in an n-dimensional space, where the distances among these points are representatives of the actual perceptual differences between them [50].

2.2   Texture Recognition Using Image Features

Surface texture refers to the micro geometry present on the surface of an object. The characteristics of this micro geometry shape the overall texture perception of the image. The micro geometry of a surface can be captured by an image. Therefore, when image features are calculated from the said image, they an reveal important characteristics of the surface texture. Image features have been widely used for classifying surfaces textures in the field of computer vision and image processing.

Haralick et al. [51–53] used Gray Level Co-occurrence Matrix (GLCM) for image texture extraction. They calculated various image features from the GLCM matrix and these features were used for classification purposes. A number of studies have shown that the GLCM features have high correlation with the texture perception ability of humans [52, 54, 55].

Amadasun et al. in [56] provided Neighborhood Gray Tone Difference Matrix (NGTDM), where the value of each pixel was the difference between that particular pixel and its surrounding pixels. It was reported that the features calculated from the NGTDM matrix are highly correlated with the human perception of surface texture.

The Gray-Level Run-Length Matrix (GLRLM) and the Gray-Level Size Zone Matrix (GLSZN) are statistical texture characterization methods [57–60]. The GLRLM counts the pixels with the same intensity in a given direction. The features calculated from this matrix are helpful in capturing the low level high frequency changes. On the other hand, GLSZM looks for pixels of same intensity in a given area. Since, image texture can also consist of relatively larger areas of the same intensity. GLSZN successfully captures this characteristic of a textured surface.

Elkharraz et al. in [61] used gradient and percentile statistics along

with other features for texture classification and later on texture genera-
tion. In [62], the authors introduced a local descriptor for capturing texture
information. They made use of filters learnt from natural images which
helped in efficient modeling. BSIF histograms were used for texture recog-
nition.

Chapter 3
84 Real Life Texture Surfaces

In order to build a comprehensive universal texture library, the textured surfaces used in the process must cover the whole range of daily life haptic interactions. The process of selecting the surfaces for the library must be thorough and well thought out. It is a well known fact in psychophysics that the larger and more versatile the dataset, the better the results. Since the aim of building the universal library is to provide image feature based automatic haptic model assignment to arbitrary surfaces, it is of utmost importance that the library contains most of the haptic models that one could possibly encounter.

One of the contributions of this research is the use of a large number of real life textured surfaces. A total of 84 different textured surfaces were used in this study. When compared to previous researches, our dataset of 84 surfaces happens to be many folds larger. For example, in [25,42] Hollins et al. used 17 surfaces in both cases, in [63] Picard et al. used 24 car seats. Similarly, Yoshioka et al. in [30] used only 16 materials. While in [64] the authors used ten papers as a dataset. However, in [44] the authors used 124 different surfaces. This is the only study known to the authors where a large number of surfaces have been used in a psychophysical experiment.

3.1   Texture Surfaces

A total of 84 real life texture surfaces were used in this study. A conscious effort was made to include most of the materials that are encountered in daily life interactions. Additionally, same materials having different kinds of textures were also used.

All the texture surfaces were cut into equal sizes of 100×100 and glued to acrylic plates of size $100 \times 100 \times 5\ mm$. The 84 real life surface textures can be seen in Figure 3.1 The broad categories of the materials used in this research are shown in Table 3.1. While, the details of all these surfaces are given in Table 3.2 and 3.3.

Table 3.1: Different kinds of materials from which the texture surfaces are made.

S. No	Material of Surfaces
1	Sponge
2	Thread
3	Wood and Cardboard
4	Paper
5	Sand paper
6	Rubber
7	Cloth
8	Metal
9	Plastic

Table 3.2: Details of the texture surfaces used in this study.

S. No	Surface Name	S. No	Surface Name
S1	Textured rubber 1	S43	Glossy paper 1
S2	Bumpy paper	S44	Glossy paper 2
S3	Textured rubber 2	S45	Wooden board
S4	Carpet 1	S46	Lined cloth 2
S5	Carpet 2	S47	Bubbly plastic 2
S6	Cotton towel	S48	Rough paper
S7	Artificial grass	S49	Smooth fabric
S8	Talc paper	S50	Hard board 1
S9	Plain cloth	S51	Lined wood 4
S10	Textured cloth 1	S52	Smooth wood
S11	Acrylic	S53	Smooth paper 2
S12	Wood	S54	Rough cloth
S13	Glitter paper	S55	Hard board 2
S14	Balloon	S56	Hard board 3
S15	Lined wood 1	557	Textured cloth 7
S16	Lined wood 2	S58	Smooth paper 3
S17	Textured cloth 2	S59	Coffee filter
S18	Bubbly plastic 1	S60	Plastic mesh
S19	Lined rubber	S61	Rough sand paper 1
S20	Rough cloth	S62	Smooth sand paper 1
S21	Slippery paper	S63	Smooth sand paper 2
S22	Carpet 3	S64	Soft hardboard

Table 3.3: Details of the texture surfaces used in this study.

S. No	Surface Name	S. No	Surface Name
S23	Aluminum foil	S65	Smooth sand paper 3
S24	Lined cloth 1	S66	Rough sand paper 2
S25	Smooth paper 1	S67	Aluminum slab
S26	Sponge 1	S68	Lined cloth 3
S27	Lined wood 3	S69	Smooth sand paper 4
S28	Textured cloth 3	S70	Textured fabric
S29	Cotton fabric	S71	Rough sand paper 3
S30	Cloth hard cover	S72	Bumpy rubber
S31	Textured shoe padding	S73	Kite paper
S32	Thick rubber	S74	Smooth shoe padding
S33	Textured rubber 2	S75	Lined wood 5
S34	Hard board	S76	Bumpy hard plastic
S35	Tissue	S77	Textured cloth 8
S36	Textured cloth 4	S78	Hairy cloth
S37	Towel	S79	Lined shoe padding
S38	Thread mesh 1	S80	Bumpy glove
S39	Textured cloth 5	S81	Steel mesh
S40	Smooth rubber	S82	Model roof tile
S41	Sponge 2	S83	Thread mesh 2
S42	Textured cloth 6	S84	Jeans

Figure 3.1: Real life texture surfaces used in this study.

3.2   Chapter Summary

In this chapter we discussed about the texture surfaces being used in this study. An effort was made to represent all type of haptic interactions, which occur in a normal day, in the surface textures that were being used here. A variety of materials including but not limited to paper, steel, cloth, metal, plastic, etc. were. These materials had different textures and perceptions as well. Thus, it is safe to say that most of the texture surfaces that a human encounters in everyday life are represented here.

Chapter 4
Perceptual Haptic Texture Space

In our daily life we can easily differentiate between different surfaces just by looking at them. For example, we are able differentiate a stone from a wood, or plastic from metal. Sometimes we can even differentiate between same materials having different textures. Nevertheless, the sense of vision is not absolute in differentiating between different textures. For example, when the difference between textures is relatively less, differentiation using mere vision becomes difficult. On the other hand, two visually similar looking surfaces can have completely different texture. Additionally, we cannot visually distinguish between hot and cold, and hard and soft surfaces most of the times. In order to counter such scenarios, we are forced to use our sense of touch. The sense of touch provides us the true nature of the surface textures. Different texture properties e.g. stiffness, roughness, friction etc can be readily judged using the sense of touch.

In order to judge differences among various surface textures based on the combined effect of the above mentioned surface properties, we conducted a psychophysical experiment. The results from this experiment were used as the ground truth for our framework.

In order to better visualize and analyze the results from the experiment, Multidimensional Scaling (MDS) analysis was performed. The MDS analysis provided us with a haptic texture perceptual space where all the surface are located in an n-dimensional space and separated from one an-

other based on the differences in their surface textures. The surfaces used
in this experiment are mentioned in Chapter 3.

4.1 Establishing Perceptual Haptic Texture Space – A Psychophysical Experiment

The purpose of conducting this experiment was to find out the differences
perceived by human subjects while interacting with various surface textures.
These differences were measured and represented in the form of a dissimi-
larity matrix. MDS analysis was performed using this dissimilarity matrix.
As a result, the locations of different texture surfaces in a 3-D perceptual
space were found.

The following subsections are dedicated towards describing the details of
the psychophysical experiment. The procedure followed in this experiment
is similar to the one followed in [42, 48]. The design of the experiment
helped in finding the perceived differences between the texture surfaces in
comparison with one another.

4.1.1 Participants and Stimuli

A total of ten human subjects participated in the experiment. Ages of the
participants ranged from 22 to 31 years. None of the participants reported
any disabilities. All the participants were right-handed. The participants
had little or no expertise in the field of haptics or regarding the current
experiment. The participants were paid for their participation.

The 84 texture surfaces described in Chapter 3 were used as stimuli in
the experiment.

4.1.2 Experimental Setup

A table was placed in front of the participants. Instructions to the participants were provided on a printed piece of paper. After reading the instructions, the participants were encouraged to ask any questions regarding the experiment. It was made sure that every participant understood the procedure pf the experiment. The participants wore a blind fold to restrict any visual cues during the experiment. They wore headphones playing pink noise. The volume of the pink noise was set to such a level that it masked the sound of interaction of hand with the surface texture, while at the same time not hindering normal conversation. The volume was optimized so that the participants could easily understand the instructions during experiment. The texture surfaces were placed in an engraved aluminum plate to avoid slipping. The experimental setup can be seen in Figure 4.1

Figure 4.1: Experimental setup for the cluster sorting experiment.

4.1.3 Procedure

Due to the large number of the texture surfaces used in the experiment, it was decided to perform cluster sorting for finding the differences among the surfaces. The advantage of cluster sorting is that it takes significantly

lesser time as compared to pair wise comparison. This ensures that the
participant does not suffer from fatigue. Additionally, the authors in [48]
show that cluster sorting can accurately capture the dissimilarities across
different texture surfaces.

In the experiment, one texture surface was provided at a time. The par-
ticipants were free to use any exploring strategy for examining the texture
surface. The participants were asked to classify the 84 texture surfaces into
perceptually similar groups. Each experiment consisted of five trials and
the total number of groups in each trial were 3, 6, 9, 12, and 15. The num-
ber of groups in a particular trial were chosen randomly to avoid any bias.
The reason behind the variable number of groups across trials was that, on
one hand, the trials with a low number of total groups ensured a broader
classification of the texture surfaces. Or in other words, textures having
even a vague perceptual resemblance were grouped together. While, on
the other hand, the trials having a higher number of total groups provided
us with groups where the samples inside a given group were perceptually
very similar. At the end of each trial, once all the texture surfaces were
classified into the given number of groups, the participants were asked to
check all the groups for any errors in classification. In case of an error,
the participants were free to reassign a given surface into another group.
The participants were free to take short breaks of five to ten minutes after
every trial. On average the experiment took 150 minutes per participant
excluding the breaks.

4.1.4 Data Analysis

In order to convert the data from the experiment into meaningful informa-
tion, a similarity matrix was formed based on the scores assigned to each
texture surface. Scores were assigned to every surface after a given trial.

Scores to a pair of surfaces being classified into the same group in any particular trial were assigned equal to the total number of groups in that trial. Afterwards, the scores for every texture surface for every participant across five trials were added together. This can be best explained with the help of some examples. If two texture surfaces were classified into the same group in four trials where the total number of groups were 3, 6, 9, and 12. Then the total similarity score for these two surfaces with respect to each other would be $3 + 6 + 9 + 12 = 27$. Similarly, if two surfaces were classified into the same group in only one trial where the total number of groups were 3, the total similarity score for such a pair would be 3. In the first example the surfaces were grouped together in four trials, thus showing that they were perceptually very similar while in the second example the pair of surfaces was grouped just in one trial signifying the fact that they were vaguely similar. The scoring scheme adopted here is designed such that the surfaces which are perceptually more similar attain a higher similarity score, which is evident from the total score assigned to each pair in the above examples.

The scores for every participant across all the trials were used to form a similarity matrix. This matrix contained the similarity scores of all the surfaces with all the other surfaces. The similarity matrices of the participants were then converted into dissimilarity matrices. The dissimilarity matrices were normalized and scaled from zero to 1000. At the end the dissimilarity matrices of all the participants were averaged to form a single 84×84 dissimilarity matrix. In the final dissimilarity matrix, a score of zero meant that the corresponding pair of surfaces were grouped together in every trial while a score of 1000 meant that they never never classified into the same group.

4.1.5 Results

Using the average dissimilarity matrix, non-metric MDS analysis was carried out. MDS analysis provides us with all the texture surfaces in an n-dimensional space where the distances among the surfaces are representative of the dissimilarity scores in the given dissimilarity matrix. In order to visualize the surfaces in a euclidean space, the number of dimensions for the MDS analysis are needed to be specified so that the distances in the euclidean space are an exact representation of the dissimilarity matrix scores. For this purpose, Kruskal stress [65] for the first ten dimensions was calculated. The stress value at dimension three is 0.05, which is considered as fair according to [49]. Additionally, the decrease in stress value beyond dimension three is not significant. The Kruskal stress values for the first ten dimensions are shown in Figure 4.2. The three dimensional perceptual space as a result of the MDS analysis is shown in Figure 4.3. Since it is difficult to follow a three dimensional graph on a two dimensional page, the two dimensional projections of the three dimensional perceptual space are also given in Figures 4.4, 4.5, and 4.6.
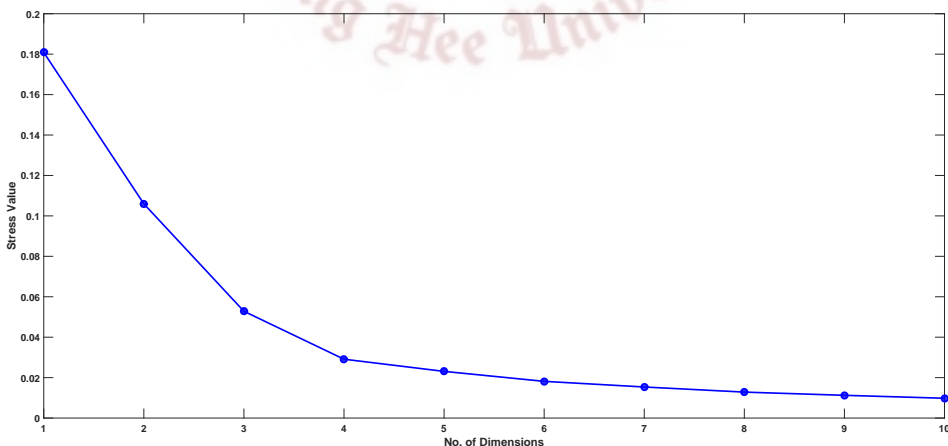
Figure 4.2: Kruskal stress values for the first ten dimensions of multidimensional scaling analysis.
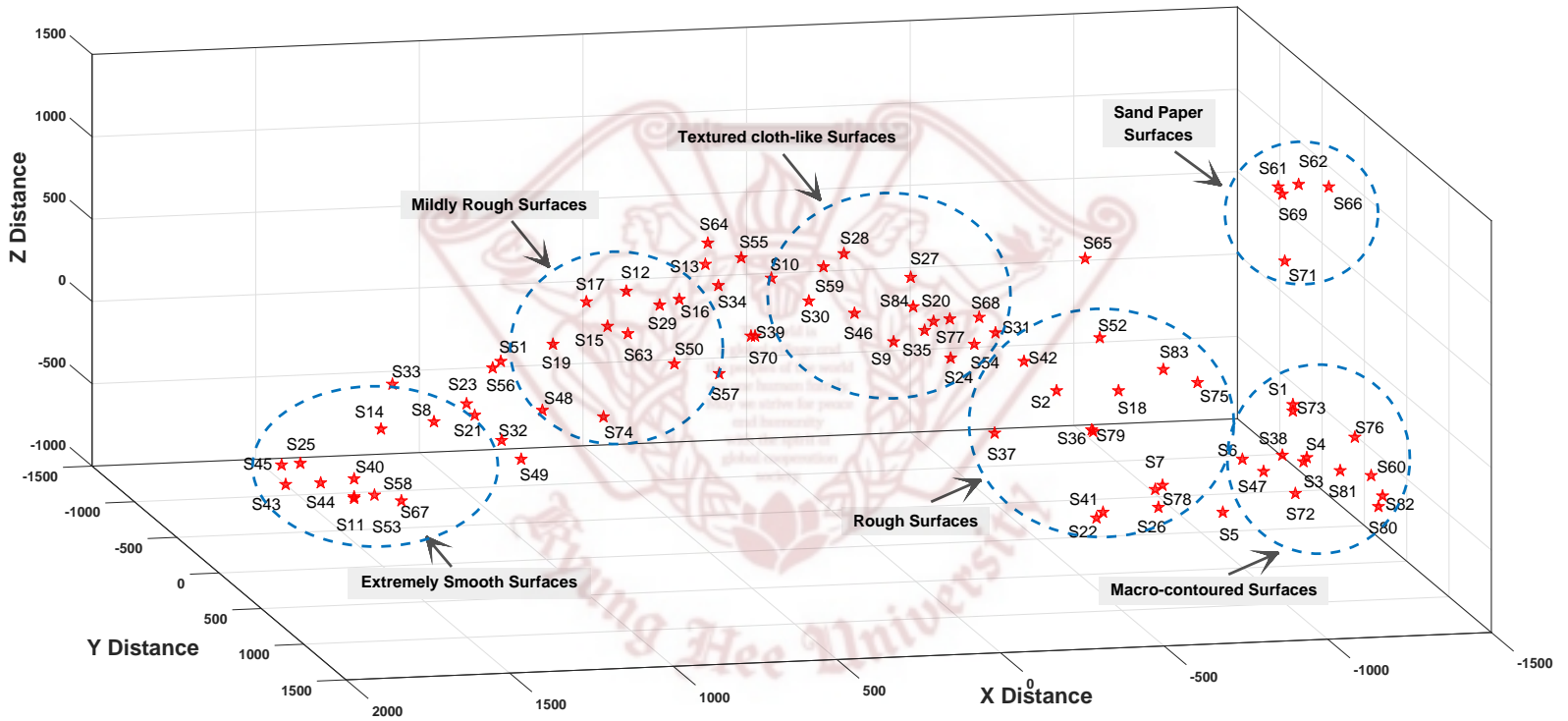
Figure 4.3: Three dimensional MDS of the haptic texture perceptual space.
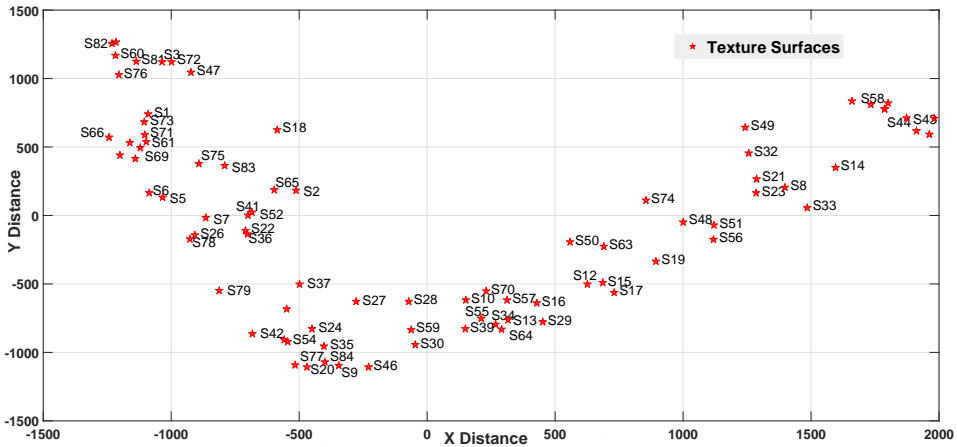
Figure 4.4: XY projection of the three dimensional haptic texture perceptual space.
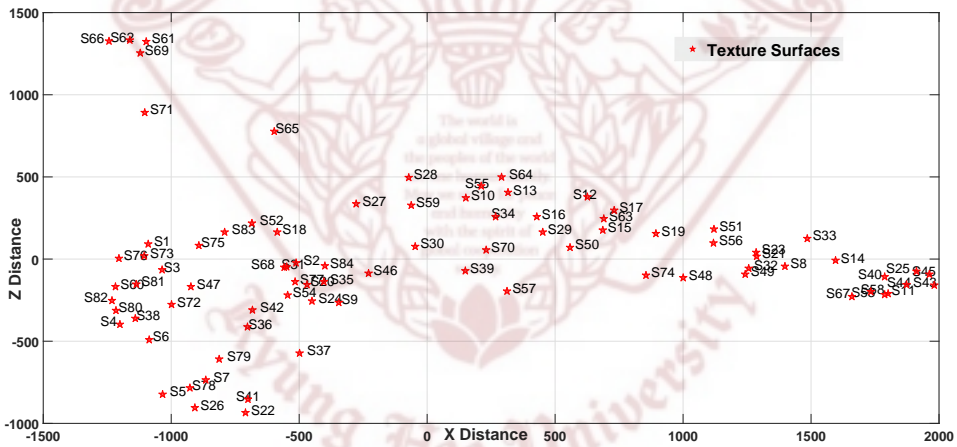
Figure 4.5: XZ projection of the three dimensional haptic texture perceptual space.

4.2   Discussion

The perceptual haptic texture space (Figure 4.3) shows some distinctive trends and groupings.   Texture surfaces having similar perception are grouped together. The scattering of the surfaces follows a horse shoe trend. The right side of the graph is occupied by the roughest surfaces. The rough-
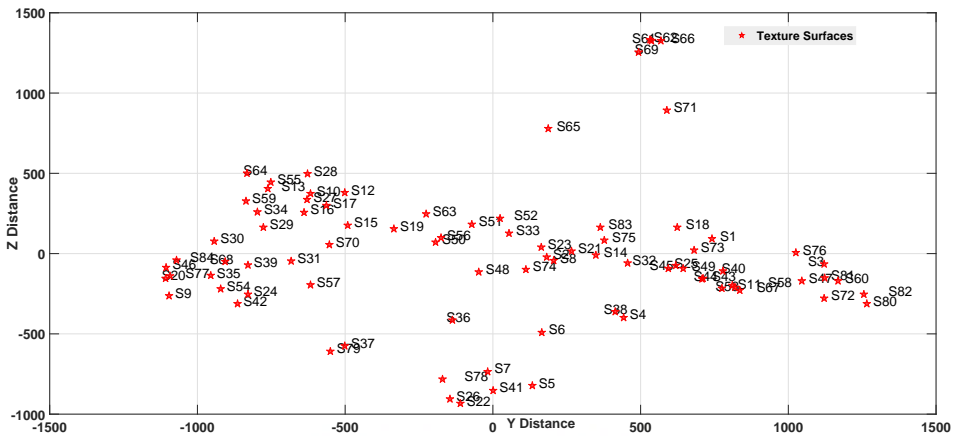
Figure 4.6: YZ projection of the three dimensional haptic texture perceptual space.

ness of the surfaces decrease as we move along the horse shoe curve towards the left side of the curve. The width of the horse shoe curve also follows a trend. The inner side of the curve tends to have softer samples as compared to the samples lying on the outside of the curve at the same location.

Upon a detailed inspection of the perceptual space, it can be seen that the sand paper surfaces are separated from all the other surfaces. They form a distinct group nearby the other rough samples. The sand paper surfaces have very distinctive properties and are easily differentiable from all other surfaces while also having a rather rough surface. Hence resulting in a very separate little cluster.

The other surfaces are placed along a continuum with a gradual decrease in the perceived roughness as we move from the right side of the curve towards the left side. The surfaces with visible contours are perceived as the roughest surfaces and occupy the right most portion of the space. Examples of the macro contoured surfaces are steel mesh (S81), plastic mesh (S60), Bumpy glove (S80), etc. Next are the surfaces with a rough surface, but where the contours are not as readily visible e.g., artificial grass (S7), bubbly

plastic (S18), lined wood (S75), etc. Moving further along the curve we encounter the cloth like surfaces which have a vivid texture. These were perceived as less rough as compared to the previous group due to the soft nature of fabrics. These include the jeans (S84), lined cloth3 (S68), lined cloth2 (S46), cloth hard cover (S30), etc. Next in line are the somewhat smooth surfaces. These surfaces do not have any visible roughness, but some texture can be felt when interaction is through touch. These surfaces are the Smooth sand paper (S63), glitter paper (S13), cotton fabric (S29), etc. Finally, the other end of the curve contains the extremely smooth surfaces. These surfaces have a very fine surface and mostly they do not contain any roughness. Examples of this type of surfaces are acrylic (S11), aluminum (S67), smooth rubber (S40), smooth paper1 (S25), etc.

In the above discussion it can be seen that the surfaces classified into the same groups are not necessarily of the same material. Plastics are classified along side steel, paper is classified with metals, etc. The only criterion on which the grouping has occurred is the similarity in perceived surface texture.

4.3 Chapter Summary

A perceptual haptic texture space was built by carrying out a psychophysical experiment. The experiment was a cluster sorting task where similarly perceived samples were grouped together by human participants. As a result of the experiment, a three dimensional perceptual space was established using MDS analysis. The perceptual space showed distinct clustering and groups of perceptually similar surfaces.

Chapter 5

Image Feature Space

In image feature space, the visual texture of a surface is described by the image feature values extracted from the image of the surface. Various researches have focused on texture recognition based on image feature values [66, 67]. Others tried to find the surface roughness, which is an integral part of surface texture, from image parameters [68, 69]. Similarly, in [70, 71] the authors used learning algorithms to estimate the roughness of a surface.

In this chapter the various image features, extracted from the images of the texture surfaces described in Chapter 3, are detailed. A total of 98 different kinds of image features are extracted from every image using well known image feature extraction techniques. Thus we have a 98 dimensional image feature vector for every image, and the image feature vectors for all the surfaces constitute our image feature space.

The main aim of this research is to predict perceptual haptic texture by using image features. Since the total number of the image features is too high, it is not feasible to use all the image features for prediction. The image feature vector was passed through a two step process to reduce its size, shown in Figure 5.1. First, a sequential forward selection (SFS) algorithm [72, 73] was applied, which provided us with the 30 best image features. Second, parallel analysis [74, 75] was run which further reduced the image feature vector to the ten best image features. These ten image features were the most correlated image features and provided the most
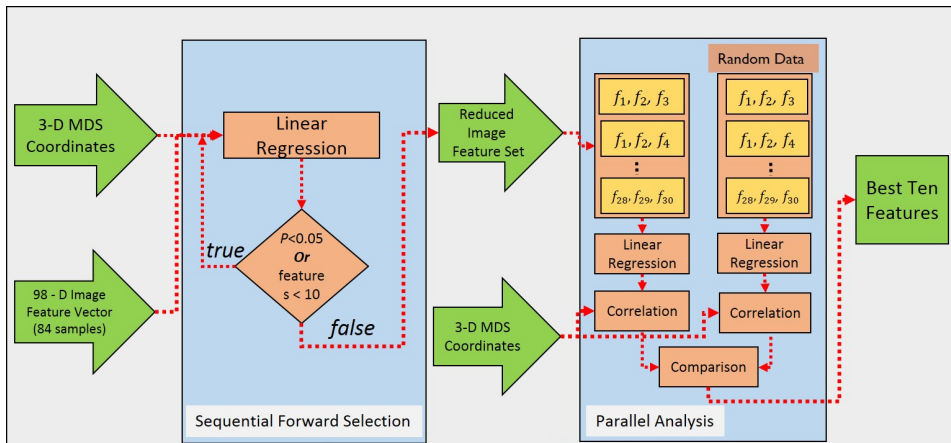
Figure 5.1: The two step feature selection process.

accurate predictions for the first three dimensions of the perceptual space.

5.1   Image Capturing Details

The finer details of an image depend on the scale and resolution of an image. In an effort to remove the effect of scaling and resolution, all images were captured from the same distance ($100mm$) using the same camera. The camera is mounted on a tripod to avoid any undesired movements of the camera. The camera used for capturing images was SIGMA Digital Camera dp2 Quattro by Sigma Corporation. It has a focal length of $30mm$, a total resolution of 33 MP, and an effective resolution of 29 MP ($5424{\times}3616$ pixels). The images were captured in high quality RAW format (loss less compression, 14-bit). Afterwards, the images were cropped to a size of $300{\times}300$ pixels. The images were also converted into gray scale, before extraction of image features, to make them color independent.

5.2 Image Feature Extraction

In order to cover every aspect of visual texture from the images, a variety of image features were extracted from every image. A grand total of 98 image features were calculated from the image of each texture surface. The details of the all the image features are provided in the subsequent subsections.

5.2.1 Gray-Level Co-occurrence Matrix Features

The methodology behind calculating the image features from the GLCM matrix was in accordance with the one defined in [51–53, 76]. The detailed explanation and formulas for extracting the GLCM features can be found in the respective papers.

The GLCM matrix is calculated by counting the number of times a specific pair of neighboring pixels have occurred across the whole image. Mathematically, the GLCM matrix $p(i, j)$ shows the number of times the gray-level pixel i occurred in neighborhood with the gray-level pixel j. The distance and direction of the neighboring pixels can be defined according to a specific purpose of use. In this study, GLCM matrices were calculated for three values of the distance parameter i.e., at 1, 2, and 4 units of distance. Additionally, the direction parameter was also varied while keeping the distance parameter constant. Every GLCM matrix was calculated for four different directions by varying the offset value to 0°, 45°, 90°, and 135°. Each set of these four matrices were then averaged together to get one GLCM matrix for every direction. Thus we had three averaged GLCM matrices calculated at distances 1, 2, and 4.

After calculating the GLCM matrices, different image features were extracted from every matrix. The image features calculated at a different distance were considered as different from one another. A total of 19 image

features were each of the three GLCM matrices. Thus we had a total of 57
GLCM image features. The details of all the image features calculated from
GLCM matrices are given in Table 5.1.

Table 5.1: Details of the GLCM features used in this study.

Gray-Level Co-occurrence Matrix Features (at d = 1, 2, and 4)	
Energy	Dissimilarity
Entropy	Contrast
Cluster Prominence	Correlation
Homogeneity	Sum of Squares
Sum Average	Sum Variance
Sum Entropy	Difference Variance
Difference Entropy	Maximum Probability
Cluster Shade	Autocorrelation
Information Measures of Correlation (1)	Inverse Difference Moment Normalized
Information Measures of Correlation (2)	

5.2.2   Gray-Level Run-Length Matrix Features

The GLRLM features were extracted based on the recommendations pro-
vided in [57–60]. For detailed implementation of the GLRLM features, the
corresponding papers can be referred.

The GLRLM matrix is calculated by counting the number of times a
specific gray-level value, spanning across a definitive length in a specified
direction, has occurred. Or in other words, the GLRLM matrix $p(i, j)$ is
the number of runs of gray level pixels i having run length j. Similar to the
GLCM matrix, the GRLRM matrix was also calculated for four different

directions i.e., 0°, 45°, 90°, and 135°, and then averaged together [61].

A total of 13 image features were calculated from the averaged GLRLM matrix. The details of these image features are provided in Table 5.2.

Table 5.2: Details of the GLRLM features used in this study.

Gray-Level Run-Length Matrix	
Short Run Emphasis	Long Run Emphasis
Gray-Level Variance	Gray-Level Nonuniformity
Run-Length Variance	Run-Length Nonuniformity
Run Percentage	Short Run Low Gray-Level Emphasis
Short Run High Gray-Level Emphasis	Low Gray-Level Run Emphasis
Long Run Low Gray-Level Emphasis	High Gray-Level Run Emphasis
Long Run High Gray-Level Emphasis	

5.2.3   Gray-Level Size Zone Matrix Features

The GLSZM features were calculated in accordance with the guidance provided in [57–60]. For detailed implementation of the GLRLM features, the corresponding papers can be referred.

The GLSZM matrix is calculated by counting the number of zones of a specific gray-level value and specific size, in any direction. Mathematically, the GLSZM matrix $p(i, j)$ represents the number of zones of gray-level pixel i and size j. The GLSZM matrix does not require to be measured in a specific direction, since by default it considers all the directions while making the zones.

Similar to GLRLM matrix, 13 image features were also calculated from the GLSZM matrix. The details of these image features are given in TableTab:GLSZM.

Table 5.3: Details of the GLSZM features used in this study.

Gray-Level Size Zone Matrix	
Small Zone Emphasis	Large Zone Emphasis
Gray-Level Nonuniformity	Zone-Size Nonuniformity
Zone Percentage	Gray-Level Variance
Small Zone Low Gray-Level Emphasis	Zone-Size Variance
Small Zone High Gray-Level Emphasis	High Gray-Level Zone Emphasis
Large Zone Low Gray-Level Emphasis	Low Gray-Level Zone Emphasis
Large Zone High Gray-Level Emphasis	

5.2.4 Neighborhood Gray-Tone Difference Matrix Features

The directions provided in [56] were used to calculate the NGTDM features. For details implementation and image features the readers can refer to the original paper.

The NGTDM matrix is calculated by measuring the difference between the gray-level value of a pixel and the average gray-level values of its neighboring pixels. mathematically, $p(i)$ is the gray-level difference between the gray-level i and the average gray-level value of its neighbors.

A total of five features were calculated from the NGTDM matrix, which are provided in Table 5.4.

5.2.5 Gradient and Percentile Features

The gradient of a gray scale image was calculated using the MAT-LAB™command *imgradient*. This command provided us with the gradient magnitude. Using this gradient magnitude, three first order statistics were calculated namely, the kurtosis, skew, and nonzero. The kurtosis and skew are self explanatory terms and need no further explanation. The nonzero of

Table 5.4: Details of the NGTDM features used in this study.

Neighborhood Gray-Tone Difference Matrix
Coarseness
Contrast
Busyness
Complexity
Strength

a matrix is percentage of the ratio of non-zero terms to the total terms in a matrix. Apart from the gradient features, a number of percentile features were also calculated.

Following [61], the three statistics from gradient along with the percentile statistics [77] were used as image features. The details of these features are provided in Table 5.5.

Table 5.5: Details of the Gradient and Percentile features used in this study.

Percentile Features	Gradient Features
Percentile 1%	Non-Zero
Percentile 25%	Kurtosis
Percentile 50%	Skew
Percentile 75%	
Percentile 90%	
Percentile 99%	

5.2.6   Spatial Frequency Feature

Spatial frequency defines the occurrence of sinusoidal components in a given material per unit area. Or, in other words, it refers to the number of tran-

sitions from high intensity (white) to low intensity (black) pixels in a given image. In order to find the sinusoidal components or the transitions in the gray scale images, fast Fourier transform (FFT) of the images was calculated. The FFT provided us with the total number of transitions in each image. Now, in order to translate these transitions into transitions per visual degree, the number of visual degrees covered by the texture surface were calculated. This was easily achieved since the actual size of the texture surfaces was known. The ratio of total transitions to the size of the texture surfaces provided us the spatial frequency of the images. The spatial frequency of the images was used as an image feature.

5.2.7   Binarized Statistical Image Features

The Binarized Statistical Image Features (BSIF) [62] is a local image descriptor which captures the texture information of an image in the form of histograms. This descriptor makes use of filters obtained from statistical properties of natural images for creating the histograms. Since, the textures in our dataset are also natural textures, therefore, BSIF was the best choice for the current study. There are two parameters in the BSIF descriptor, the filter size and the bit length of each string. For the current study, a filter size of 15×15 and a string length of 12 bits was experimentally selected. The BSIF features were calculated for all the 84 texture surfaces in the form of histograms.

BSIF features are not part of the image feature vector, instead they are used as part of the automatic haptic model assignment process (discussed in Chapter 6).

5.3   Image Feature Selection

A grand total of 98 image features were calculated from the image of each texture surface. All these image features are reported to capture various aspects of surface texture and thus none of them can be deemed as insignificant before thorough testing. But given the large size of the image feature vector (98 image features), it was not feasible to incorporate all the image features.

For this purpose, the image feature vector was subjected to a two step wrapper based image feature selection process. In the first step, the image features most correlated with the first three dimensions of the perceptual space were selected through a Sequential Forward Selection (SFS) algorithm. The SFS gave us the best 30 image features from the set of 98.

In the second step, these 30 image features were subjected to a Parallel Analysis (PA) test to check whether the correlation values in SFS were achieved by chance or they bare some significance. The best ten image features according to the PA test, with the highest predictive ability with respect to the first three dimensions of the perceptual space obtained from MDS analysis, were selected at the end of the process.

5.3.1   Sequential Forward Selection

The basic concept of the sequential search algorithms is that they add or remove features one at a time. In forward selection, they start with an empty set and iteratively add one feature to the set until the termination criterion is met.

In this study, a sequential forward selection algorithm was used to reduce the dimensionality of the image feature vector. The input to the algorithm was the vector comprising of the 98 image feature for all the 84 texture

surfaces. The most correlated subset of the image feature vector which showed the highest predictive ability towards the first three dimensions of the perceptual space had to be selected.

The algorithm considers one dimension of the perceptual space at a time. For every single dimension of the perceptual space, the algorithm starts with the most correlated image feature. A linear regression model is built from this image feature, which is used to predict the same dimension. The algorithm then adds a second image feature together with the old one and predicts the associated dimension of perceptual space. This process is repeated until a predefined termination criteria is being met. The termination criteria in this case is either of, the prediction error being significantly reduced i.e., $pvalue = 0.05$ using partial F-test, or a total of ten image features being selected. The total number of ten image features was empirically selected. Additionally, ten image features were considered sufficient to explain the variability along one dimension of the perceptual space. These steps were repeated three times to obtain the best image features for the first three dimensions of the perceptual space.

It was seen that the predictive error for all three dimensions never reduced significantly for the first ten most correlated image features. None of the individual features were selected for more then one dimension, all ten features of every dimension were different. Therefore, a total of 30 image features were selected at the end of the sequential forward selection process. The prediction errors for most correlated ten image features for their respective dimensions is shown in Table 5.6.

5.3.2   Parallel Analysis

Parallel analysis is one of the most accurate methods for factor retention [78, 79]. While in [80] Glorfeld claimed that there is little reason to

Table 5.6: P-values of upto ten image features for the first three dimensions of MDS using partial F-test. None of the values are greater than 0.05. While, only the three bold face values are greater than 0.01.

Number of	p-value		
Image Features	Dimension 1	Dimension 2	Dimension 3
1	9.02e-07	2.70e-09	0.0003
2	3.33e-06	2.11e-08	0.0003
3	6.09e-08	1.01e-07	0.0008
4	1.19e-07	3.87e-07	0.002
5	1.37e-07	2.13e-07	0.003
6	4.33e-07	5.90e-07	0.006
7	1.10e-06	1.21e-06	0.007
8	1.10e-06	4.11e-08	**0.012**
9	2.23e-06	1.17e-07	**0.021**
10	2.30e-06	2.69e-07	**0.01**

use any method other than PA for factor retention. In PA the important or significant factors are retained by comparing the predictive ability of the real dataset with that of a randomly generated dataset having the same dimensions as the real one.

In the current study, the predictive ability of the reduced image feature set of 30 image features was compared against the predictive quality of a randomly generated data matrix. It was assumed, if there exists a relationship between the image features and the perceptual space, the predictive quality of the image features should be higher than that of the random data.

The reduced image feature set was further divided into subsets of three image features. The predictive ability of each of these subsets was tested by predicting the first three dimensions of the perceptual space. Similar to

the SFS, the perceptual space dimensions were considered one at a time. Prediction was done using a linear regression model. The output from the regression model was the predicted co-ordinates of the surfaces in the respective dimension of the perceptual space. As a next step, the correlations, between the predicted values of a specific dimension and the actual values of the perceptual space dimension, were measured and stored.

At the other hand, a random data matrix was generated which had the same number of columns and the same number of rows as the reduced image feature set. The randomly generated matrix was also divided into subsets of three, which were used to predict the first three dimensions of the perceptual space. The correlation values between the predicted and actual dimensions were recorded.

It must be noted that the correlation values measured from the random data matrix are the values which can be achieved by chance and bare no significance. The correlation values of the reduced image feature set should be higher than those achieved by the random data matrix [81,82]. Therefore, only those feature subsets of the reduced image feature set can be deemed significant which show a correlation value higher than that of the random data matrix. The correlation values for the subsets of reduced image feature set (see green bars) and random data matrix (see red bars) are shown in Figure 5.2.

As shown in Figure 5.2, the maximum correlation value for a random data matrix subset is 0.47. For a more robust result, a value of 0.5 was considered instead of 0.47. Going forward, only those feature subsets are considered significant which show a correlation value higher than 0.5. Since our requirement is to select the best features while every feature subset consisted of three image features, the frequency of occurrence of a particular image feature in the significant feature subsets was calculated. The best

image features were the ones which occurred most often in the significant feature subsets. As a result of this exercise, ten image features with the highest frequency were selected as the best image features. The best ten image features are provided in Table 5.7. These image features will be used in the automatic haptic model assignment, which be discussed in the upcoming chapters.

Table 5.7: The best ten image features obtained as a result of sequential forward selection and parallel analysis.

No.	Image Feature
1	Gray-Level Non-Uniformity (GLRLM)
2	Gray-Level Non-uniformity (GLSZM)
3	Small Zone High Gray-Level Emphasis (GLSZM)
4	Percentile 25% (Percentile)
5	Correlation (GLCM at d = 4)
6	Homogeneity (GLCM at d = 4)
7	Information Measure of Correlation (2) (GLCM at d = 4)
8	Inverse Difference Moment Normalized (GLCM at d = 4)
9	Homogeneity (GLCM at d = 2)
10	Information Measure of Correlation (1) (GLCM at d = 2)
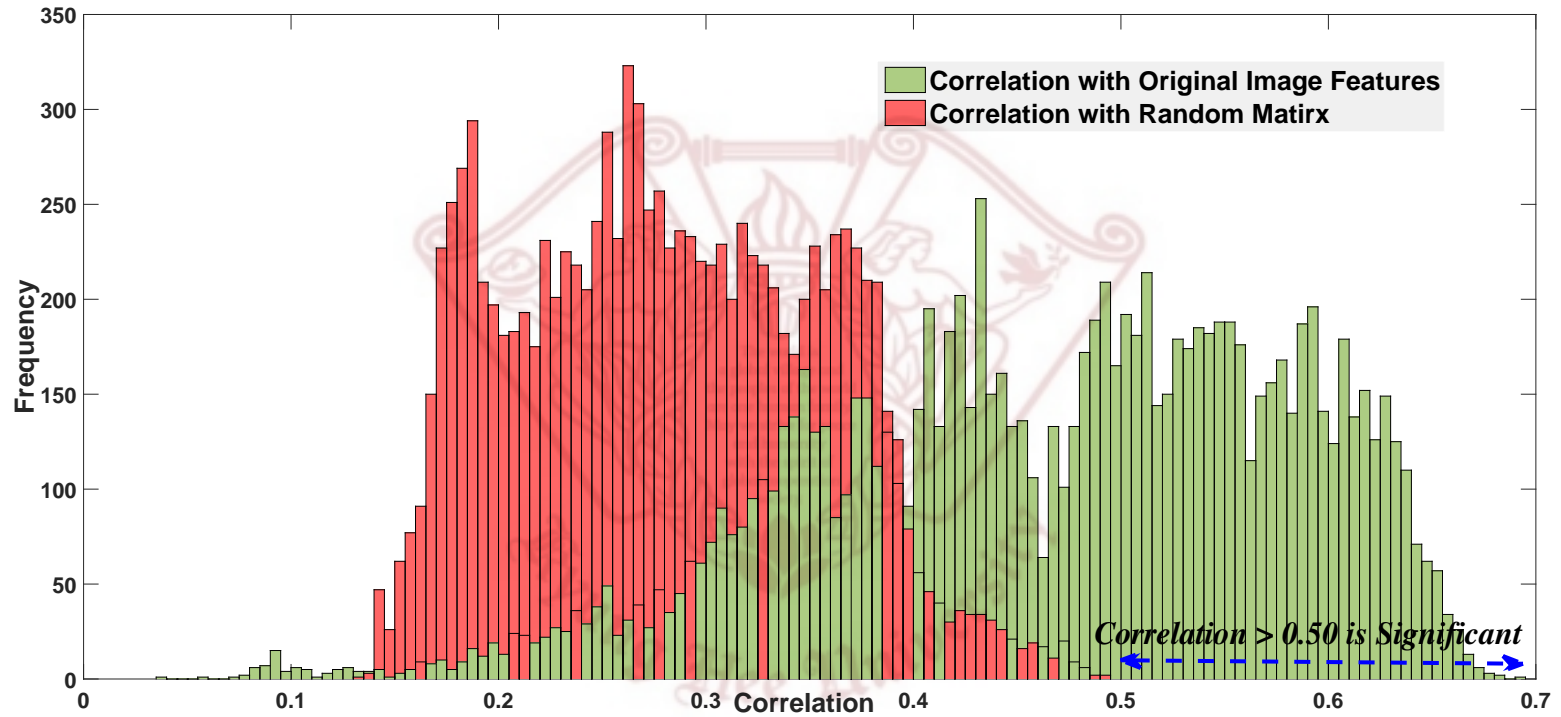
Figure 5.2: Correlation values of the reduced image feature subsets (30 image features) and the randomly generated data matrix subsets with the first three dimensions of the perceptual space.

5.4 Chapter Summary

This chapter describes the details about extracting image features from the images of the texture surfaces mentioned in Chapter 3. A total of 98 different image features were calculated from each image. The image feature vector was then progressively reduced to select the best image features which are most correlated with the perceptual space. A wrapper based selection methodology was applied for the reduction of image features. Sequential forward selection and parallel analysis techniques were part of the wrapper methodology. At the end of the selection process, the image feature vector was reduced to a total of ten image features.
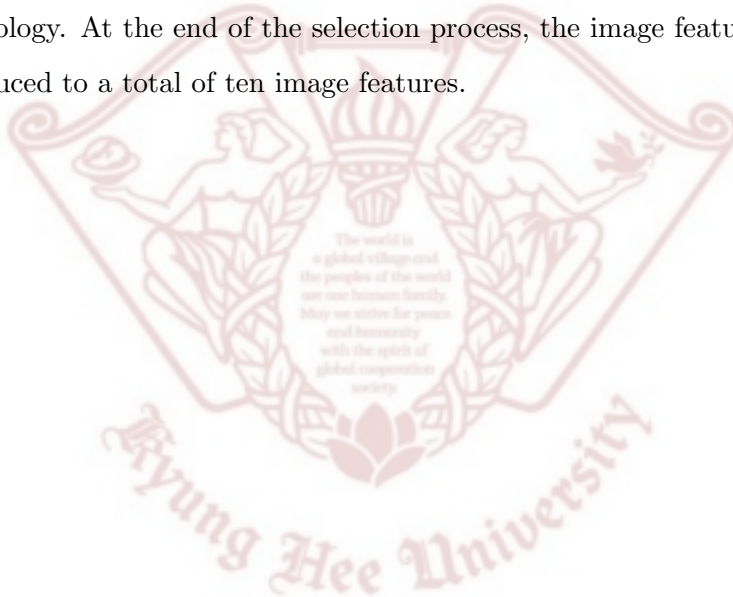
Chapter 6
Automatic Haptic Model Assignment

The main aim of this study is to find a relationship between visual image texture and perceived haptic texture. And then use that relationship to build a library from where haptic models could be assigned to new - outside library - texture surfaces based on their image features alone. For accomplishing this aim, a perceptual haptic texture space and an image feature space has been established. As discussed in Chapter 4, the perceptual space showed distinct groupings of perceptually similar texture surfaces. While, in Chapter 5, it was substantiated that the image feature space showed some relation with the perceptual space. Based on this knowledge, it can be assumed that the image feature space can also be classified into groups of perceptually similar images.

For this purpose, a one-versus-rest Multi-Class Support Vector Machine (MC-SVM) [83] in conjunction with the K-means algorithm was used for classifying the image feature space. Once MC-SVM model was trained using the already established perceptual and image feature spaces, it was readily used for classifying newly encountered texture surfaces into perceptually similar clusters of the image feature space. Subsequently, a unique match to the new texture surface was assigned using Binarized Statistical Image Features (BSIF) [62].

6.1 Relationship Between Perceptual Haptic Texture Space and Image Feature Space

Since, the distribution of the images in the image feature space could not be identified, it was not feasible to use simple classification techniques which deal with linearly separable data. In this study our requirement was a classification method which could seamlessly handle both linearly separable and inseparable data. A space in which data clusters can be separated linearly is called as linearly separable space.

6.1.1 Training Multi-Class Support Vector Machine

Support Vector Machine (SVM) algorithms have been widely used in lter-ature for binary classification [84–87]. But, in the current study, our aim is to classify the image feature space into multiple perceptually similar clusters. For this purpose, a one-versus-rest MC-SVM was used similar to ones used in [88–90] A simple MC-SVM can work very well when data are distributed into fairly differentiable clusters. But, if the data clusters are diffused into one another, as might be the case in the image feature space, a simple SVM classification can be misleading and erroneous. Therefore, the MC-SVM was used in conjunction with the a Radial Basis Function (RBF) kernel for clusterizing the image feature space [91, 92]. The parameter $sigma$ was experimentally tested for different values and the best results were obtained at $sigma = 4$.

For training the MC-SVM model, we need the input data to be classified and class labels for these data. The reduced image feature set of ten features for all the 84 texture surfaces was used as an input for training the MC-SVM model. While, for providing class labels for these data, K-means algorithm [93] was used for clusterizing the haptic texture perceptual space

and to classify the surface textures into groups. As reported in Chapter 4, perceptually similar surfaces were located in close proximity to one another, therefore, the K-means classification provided us with groups having perceptually similar texture surfaces. Thus, the labels provided to the MC-SVM were based on perceptual similarity of the texture surfaces. In the K-means algorithm, the value of k was subjectively decided to be 16. Since, the overall range of surfaces used in this study can be broadly classified into 16 categories. The perceptual space after the K-means clusterization can be seen in Figure 6.2. The imbalance in the variance of the groups increases if the total number of groups are increased beyond 16. While, a lower number of total groups results in perceptually different surfaces being grouped together.

As a result of this exercise, the image features were labeled from perceptual clusterization and the MC-SVM was trained on this data. Consequently, a *Haptic Texture Library* was formed where image features of texture surfaces were directly associated with the perceptual haptic texture of the surfaces. The trained model of MC-SVM was used to classify new texture surfaces to perceptually similar groups based on the image features of the new surface.

6.2   Automatic Haptic Model Assignment

The automatic haptic model assignment is a two step process, as shown in Figure 6.1. First, the trained MC-SVM model is used to classify the newly encountered texture surface into a perceptually similar group based on its image features. Second, a unique match for the new surface from within the group is found using BSIF features, an image based classification technique.

The reduced image feature set of ten image features is calculated for the
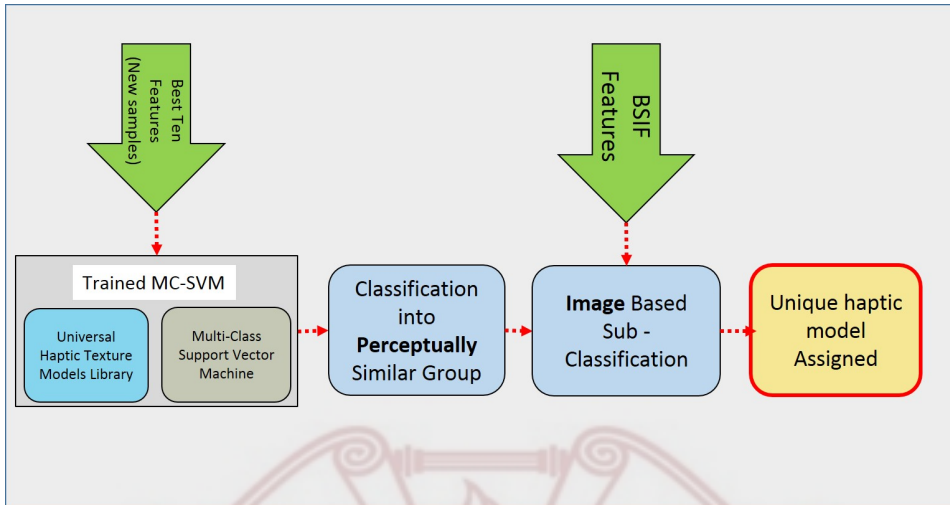
Figure 6.1: The process of automatic assignment of haptic models to new texture surfaces in the perceptual space.

new surface, which is then used as a test input to the trained MC-SVM model. Using the image features, the trained MC-SVM model classifies the new surface into one of the groups. This texture surfaces in this group are considered as perceptually most similar to the new surface.

The BSIF features for all the texture surfaces in the library are already extracted and stored. After the new surface is classified into one of the groups, its BSIF features are calculated and compared to all the surfaces within the selected group. The haptic model of the texture surface, within the group, which is closest to the new surface is selected and assigned to the new surface. The closest match is found using the chi-squares distances.
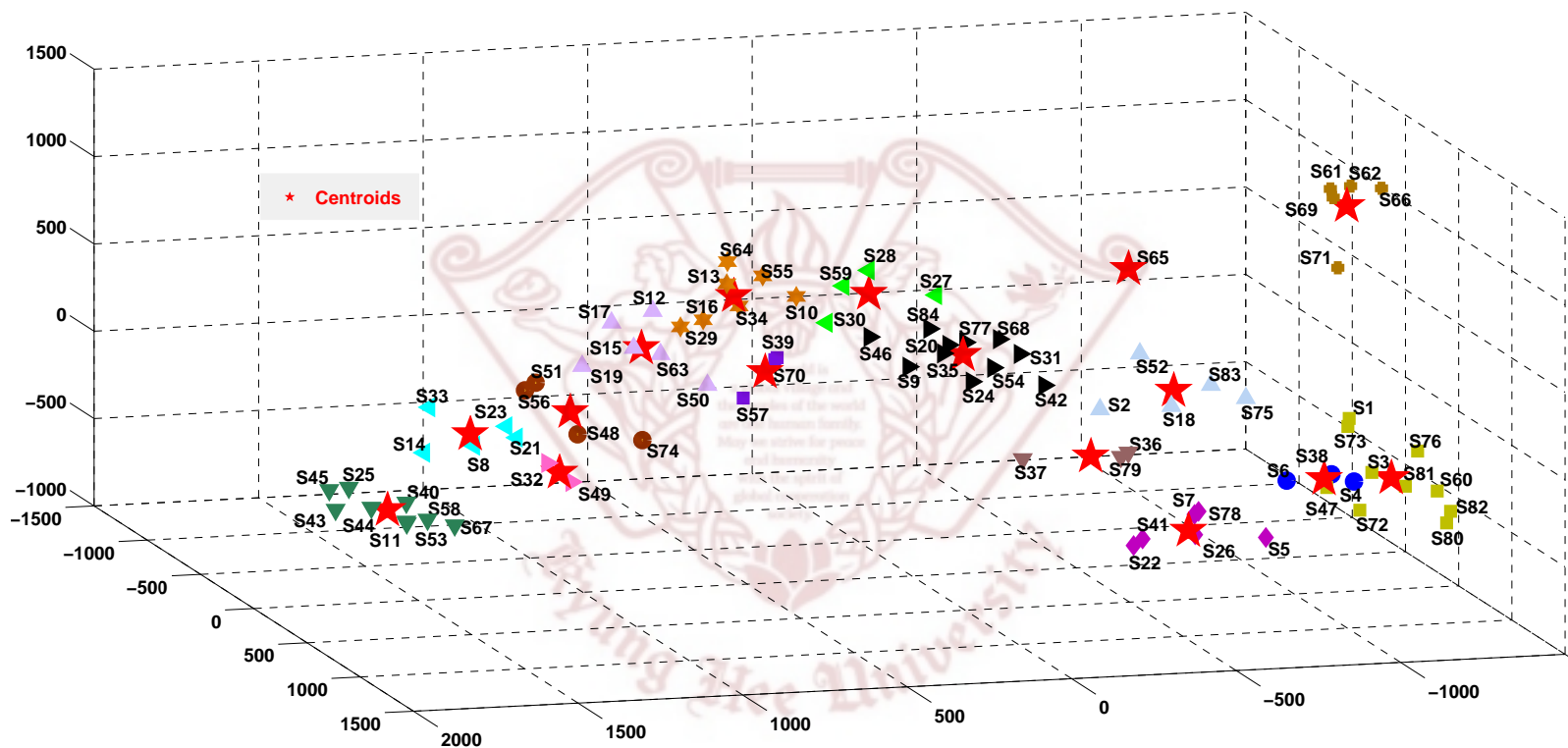
Figure 6.2: Three dimensional MDS of haptic perceptual space. The different colors (and shapes) represent the different groups as a result of K-means clustering. The stars show the centroids of the groups.

6.3   Chapter Summary

This chapter details the process of automatic haptic model assignment. A relationship between haptic texture perceptual space and the image feature space was established using a one-versus-rest MC-SVM with and RBF kernel in conjunction with K-means clustering. This relationship was a first step in automatic haptic model selection process. It was used to assign new texture surfaces into perceptually similar texture groups. Afterwards, a unique match for the new surface was selected using BSIF features.

Chapter 7

Evaluation

A new set of 21 real life texture surfaces were used to evaluate the algorithm. The algorithm assigned haptic texture models to the new surfaces. In order to cross check if the haptic models assigned by the automatic haptic model assignment algorithm are truly perceptually the best models for the new surfaces, a psychophysical experiment was designed.

The new texture surfaces along with the old ones (84 surfaces) were used in the experiment. A new perceptual space was established using MDS analysis. The purpose of the experiment was to find out the location of the new surfaces with respect to the old ones in the perceptual space. The locations of the new surfaces in the new perceptual space were used to examine the validity of the automatic assignment algorithm.

7.1 Psychophysical Experiment

The experiment was a cluster sorting task similar to the one in Chapter 4. The details of the experiment are given in the following sub-sections.

7.1.1 Participants

Six participants took part in the experiment. They were paid for their participation. None of the participants reported any disabilities. All the participants were right handed. None of the participants in this experiment
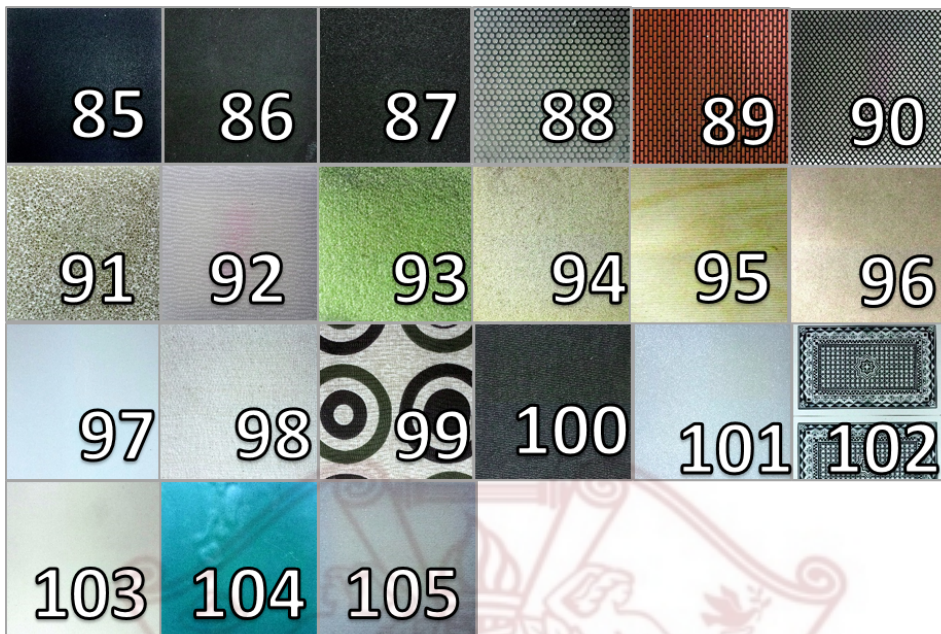
Figure 7.1: New textured surfaces used for evaluation.

were part of the previous experiment. The participants had little or no knowledge about the procedure of this experiment or haptics in general.

7.1.2   Stimuli

A total of 105 real life texture surfaces were used in this experiment. A new set of 21 real life texture surfaces were used in addition to the 84 texture surfaces mentioned in Chapter 3. The new sample were also mounted on acrylic plates of size 100×100×5 mm. The new set of texture surfaces is shown in Figure 7.1, while their details are provided in Table 7.1.

7.1.3   Procedure

The experiment was a cluster sorting task where participants were asked to classify the texture surfaces into perceptually similar groups. Each partici- pant had to conduct three trials. The total number of groups per trial were

Table 7.1: Details of the new textured surfaces used for evaluation.

S. No	Surface Name	S. No	Surface Name
85	Smooth sandpaper	96	Hard board
86	Rough sandpaper	97	Gift Card
87	Very rough sandpaper	98	Towel
88	Steel mesh 1	99	Textured cloth 1
89	Model brick	100	Textured cloth 2
90	Steel mesh 2	101	Styrofoam
91	Abrasive sponge	102	Playing cards
92	Lined plastic	103	Hard cover
93	Scrub	104	Glossy plastic
94	Sponge	105	Bandage
95	Lined wood		

6, 9, and 12. The order was randomly selected across participants to remove ordering bias. The participants were not informed about the inclusion of a new set of texture surfaces. They treated all the surfaces as new. The rest of the experimental details and experimental setup was the same as the one discussed in Chapter 4. Total time for one participant was around 150 minutes.

7.1.4   Data Analysis and Results

After the experiment, scores to the surfaces were assigned in a similar manner to the experiment in Chapter 4. The scores were used to form a dissimilarity matrix and then scaled from zero to 1000. A score of zero meant that the two surfaces were perceptually similar, while a score of 1000 meant that the two surfaces were perceptually opposite to one another and were never

classified into the same group in the experiment. In order to visualize the dissimilarity scores in the form of a space, MDS analysis was performed on the dissimilarity matrix. A new three dimensional space was established. In this space the new surfaces were located in addition to the old surfaces.

The space established as a result of the above exercise was also clustered into 16 groups using K-means clustering. The new space after K-means clustering can be seen in Figure 7.2.

7.1.5   Evaluation Criteria

On one hand, the automatic haptic model assignment algorithm was used to assign haptic models to the new texture surfaces based on their image features. On the other hand, in the experiment, the participants classified the new texture surfaces to different groups along with the old texture surfaces. After applying K-means to the new space, made up of the combination of the 21 new surfaces and 84 old ones, all the surfaces were classified into perceptually similar groups. The new textured surfaces also appeared in these groups along side the old surfaces. These groups would work as the ground truth for the automatic haptic model assignment algorithm. An automatic assignment of a haptic model would be deemed as correct only if both the new surface and the corresponding assigned model appeared in the same perceptual group in the new space.

Based on this strategy, the haptic models assigned to all the new surfaces evaluated. A total of 15 out of the 21 new surface texture were assigned perceptually correct models i.e., the new texture surface and corresponding assigned model were in the same perceptual group. The haptic models assigned to the 21 new texture surfaces are presented in Table 7.2. Figure 7.2 highlights the new texture surfaces and the corresponding assigned models inside the new perceptual space.

Table 7.2: Haptic textures models assigned to the 21 new texture surfaces used for evaluation.

New Texture Surface	Assigned Model	Remarks
85	30	Correct
86	26	Correct
87	61	Correct
88	47	Correct
89	60	Correct
90	76	Correct
91	73	Correct
92	73	Correct
93	7	Correct
94	7	Correct
95	73	Wrong
96	21	Wrong
97	50	Correct
98	7	Correct
99	24	Correct
100	66	Wrong
101	13	Correct
102	72	Wrong
103	48	Correct
104	61	Wrong
105	43	Wrong
Average correct classification rate		**71.4%**
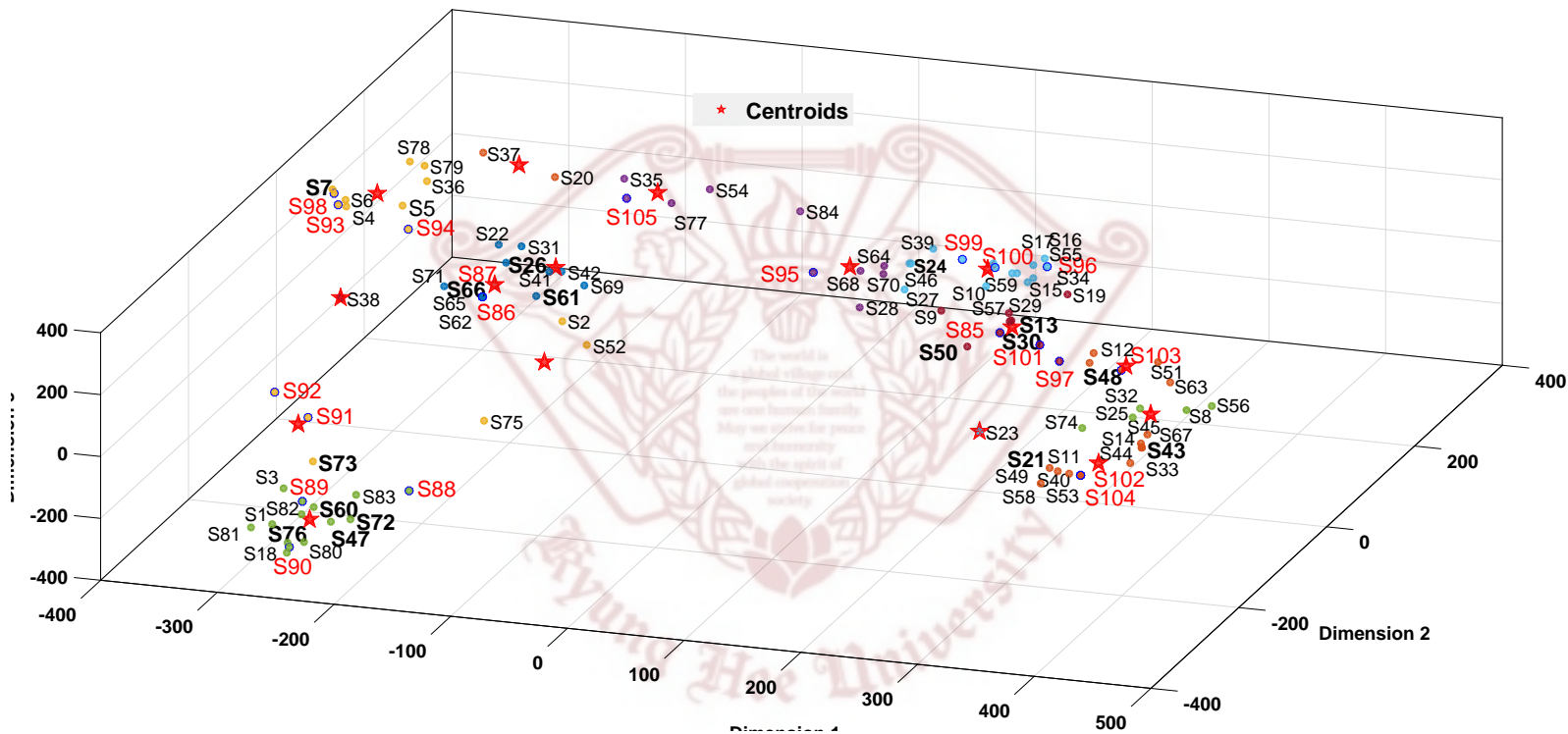
Figure 7.2: The new perceptual space made up of 21 new and 84 old texture surfaces. The different colors represent the different groups as a result of K-means clustering. The stars show the centroids of these groups. The new surfaces are written in red color while the assigned models are shown in bold black color.
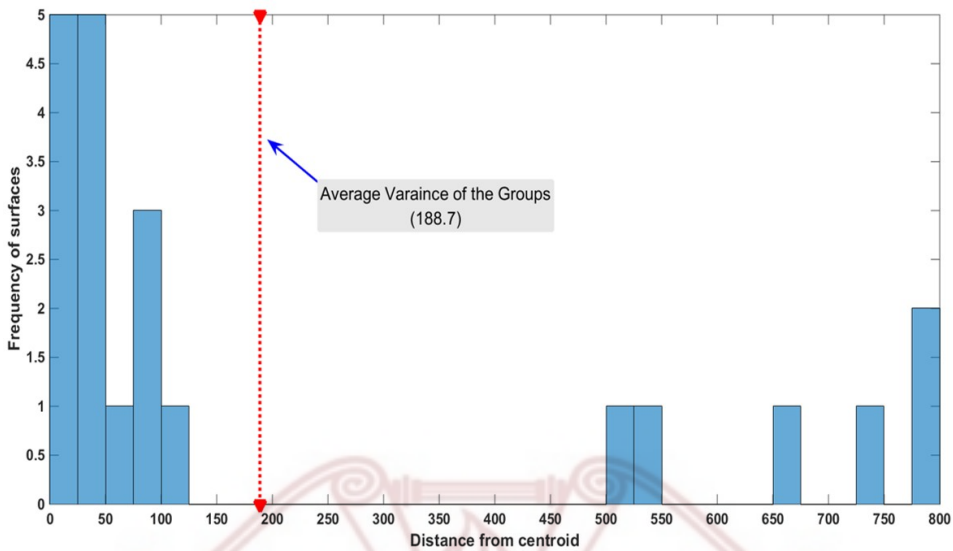
Figure 7.3: Histogram of the distances between new surfaces and the assigned haptic models from the library.

After checking for the correct perceptual group assignment, it was important to check if the assigned models and new texture surfaces appear closer to each other inside a group or not. This closeness was checked in relation to the overall variance. The variance of all the perceptual groups was calculated and averaged out. The average variance of all the groups was 188.7 units. Based on this variance, the new surfaces having smaller distances as compared to average variance are considered as perceptually very similar to their assigned model from the library. The distances histogram in Figure 7.3 shows the majority of the surfaces exhibit far less distances as compared to the average variance. This means that the majority of assigned models are perceptually very similar to the new surfaces.

7.2 Discussion

From Figure 7.2, it can be seen that texture surfaces having visible contours (S88, S89, S90 etc.) or the ones having some degree of roughness in texture (S86, S87, S93 etc) are quite accurately classified. The image features from these surfaces were very clear and the algorithm could readily differentiate the surfaces from one another. On the other hand, the smooth surfaces (S102, S104) were incorrectly classified due to the fact that the images captured from these surfaces could not portray the surface micro geometry. This can be accredited to the limitation of hardware since the camera could not capture the surface details for these texture surfaces. Thus the image features from these surfaces were not clear and the algorithm classified them incorrectly.

Another set of surfaces that was wrongly classified was the set of S100 and S95. S100 was assigned a moderately rough sandpaper (S66). Upon a closer inspection it was revealed that the actual surface texture of the two surfaces was quite similar and that the two should have been assigned to the same group, while building the actual perceptual space, by the human subjects. Same was the case for S95 which was assigned S73. These two also resemble each other and should have been placed in the same group.

After careful deliberation on the experimental process it was noted that since S66 was a sandpaper and as soon as it was encountered, human subjects would directly assign it to the group where other sandpapers were previously placed. This assignment usually took place without considering the actual surface details, instead the basis for assignment were the material properties of the surface. Additionally, sandpapers have a very peculiar surface and are easily recognizable. This fact also aided the material based assignment process. At the same time, S100 was equally rough but it was a

fabric. The face that it was a fabric played a major role in it being assigned to a completely different as compared to the said sandpaper.

The phenomenon where surfaces were classified based on their material properties instead of actual textural differences has been called as *Pre-Judgement* in this study. In pre-judgment participants used their previous knowledge for classifying a said surface. A similar scenario developed for the S95 and S73 pair, where S95 was a wood (a classic case of pre-judgement) and S73 was a kite paper. Further details about pre-judgement are provided in Chapter 8.

7.3   Chapter Summary

In this chapter the automatic haptic model assignment algorithm was evaluated using 21 new real life textured surfaces. A psychophysical experiment was conducted to authenticate the validity of the algorithm. A new perceptual space was built using the 21 new texture surfaces and the 84 old ones. The algorithm correctly classified 71.4% of the new texture surfaces by assigning perceptually the most similar haptic model.

Chapter 8

Perceptual Differences Between Bare-handed and Tool-Based Interaction

In Chapter 7 it was shown that participants used pre-judgment in evaluating texture surfaces while using bare hands. This led us to explore if pre-judgment is a property associated with bare handed interaction or can it also occur in the tool based interaction. Another motivation for this study was the fact that most rendering environments provide tool based haptic feedback, which is contrary to our every day experience where we use bare hands for interacting with different objects.

The main focus of this chapter is to evaluate the perceptual differences between bare handed and tool based interaction with texture surfaces. For this purpose, perceptual spaces were established for both modes of interaction using a cluster sorting experiment. A total of 31 texture surfaces were used, a subset of the texture surfaces used in Chapter 3. Additionally, an adjective rating experiment was also conducted which helped in quantifying the differences in the perceptual space by comparing the affective properties of the texture surfaces.

8.1 Experiment - Perceptual Space

The first experiment was a cluster sorting task similar to other experiments carried out in the previous chapters. The details of the experiment are given

in the following subsections.

8.1.1   Participants and Stimuli

A total of six participants took part in the experiment. All participants were males except one. They reported no disabilities. Their ages were between 23 and 30 years. They were paid for their participation.

The stimuli used in this experiment were 31 real life texture surfaces. These 31 surfaces were a subset of the 84 texture surfaces discussed in Chapter 3. It was not feasible to use all the 84 surfaces in this study. Therefore, the surfaces for this study were selected in such a way that all the different kinds of textures present in the set of 84 surfaces were sufficiently represented. The 31 texture surfaces are given in Figure 8.1 and their details are provided in Table 8.1
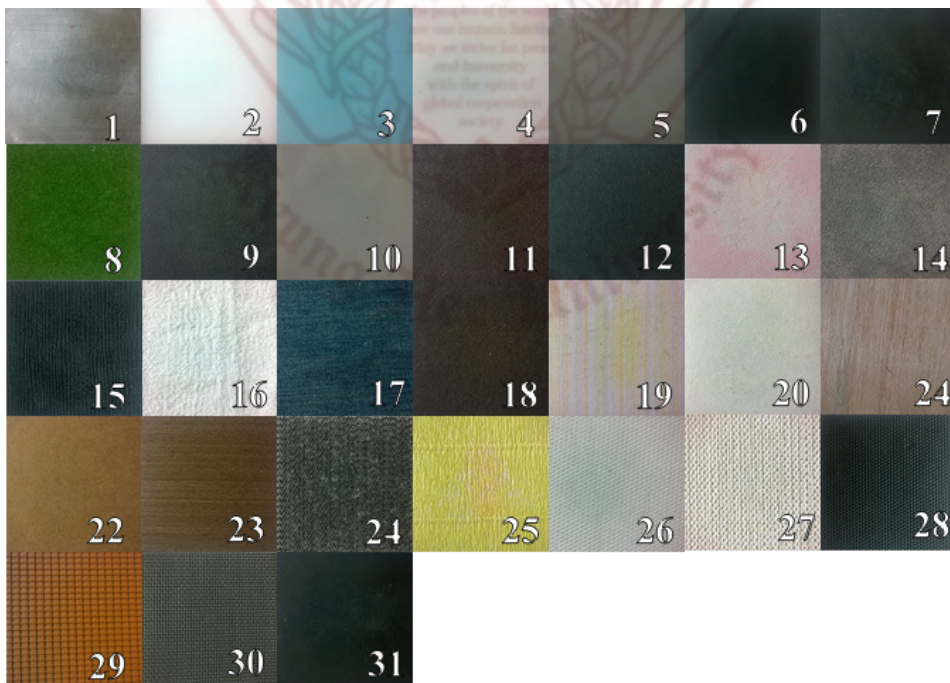
Figure 8.1: The real life surfaces used in the experiment

.

Table 8.1: Details of the 31 surfaces used in this study. *The average particle size of the sandpapers.

S. No	Surface Name	S.no	Surface Name
1	Aluminum	17	Jeans
2	Acryl	18	Rough cloth 1
3	Sandpaper (1 mm)*	19	Rough cloth 2
4	Glossy paper	20	Wet tissue
5	Thin rubber	21	Lined Wood
6	Lined rubber	22	Hard board
7	Thin rubber	23	Lined Wood
8	Artificial grass	24	Thread mesh
9	Sandpaper (36 mm)*	25	Lined Kite paper
10	Sandpaper (6.5 mm)*	26	Textured shoe pad
11	Sandpaper (192 mm)*	27	Textured rubber
12	Plywood	28	Textured hard rubber
13	Textured Cloth	29	Model Roof tile
14	Contoured cloth	30	Steel mesh
15	Thick cloth	31	Thick rubber
16	Towel		

8.1.2 Procedure

The experimental setup used in this experiment was similar to the ones carried out in Chapter 4. Figure 8.2 shows the setup for this experiment.

The experiment was a cluster sorting task where participants were asked to classify the given 31 texture surfaces into perceptually similar groups. They were provided one sample at a time. A total of three trails were conducted per participant. Since the total number of texture surfaces was

not very large, the total number of groups per trial were 3, 6, and 9. After classification of all the surfaces, the participants were given a second chance to check for any mistakes in classification.

The experiment was separately conducted for bare handed and tool based interaction. The order of the two modes was reversed across participants to avoid ordering bias. In the bare handed interaction, the participants were allowed to use their index finer. In the tool based interaction, the interaction was through a rigid aluminum tool in the shape of a pen. The tip of the tool was hard plastic having a diameter of 7 mm and a length of 14 cm. The tool can be seen in Figure 8.3. The choice of scanning strategy was given to the participants.

8.1.3 Data Analysis

The experimental data was converted into a similarity matrix using the scoring system discussed in Chapter 4. Later on the similarity matrix was converted into a dissimilarity matrix and scaled from zero to 1000. We calculated separate dissimilarity matrices for both modes of interaction.

8.1.4 Results

The dissimilarity matrices was converted into two different perceptual spaces by scaling them with MDS. The Kruskal stress values for both the perceptual spaces are given in Figure 8.4. From the figure we can see that at dimension four the values of stress for bare handed and tool based interaction are 0.12 and 0.15, respectively, which are considered are fair according to [49]. Therefore a four dimensional perceptual space was established for both modes of interaction. Since, we can not represent four dimensions on a paper, two two-dimensional projections of the perceptual space were made. As we have to compare the two perceptual spaces, they are shown together

Figure 8.2: The experimental setup and environment for the experiment. Top is tool based interaction, bottom is bare handed interaction.
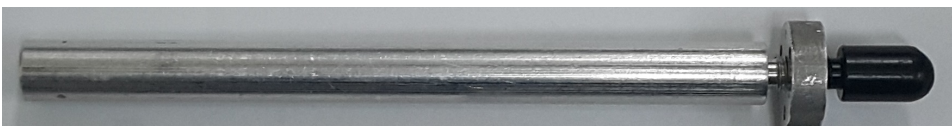
Figure 8.3: The aluminum tool which is being used for interaction in tool-based interaction. Its has a tip diameter of 7 mm, and a total length of 14 cm.
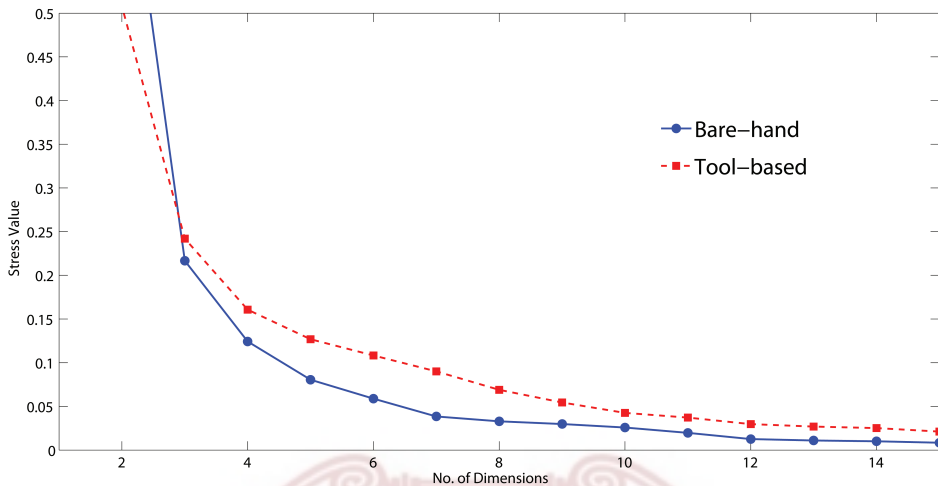
Figure 8.4: Kruskal stress for the first fifteen dimensions of both the perceptual spaces.

in Figures 8.5, Figure 8.6. Figure 8.5 shows the first two dimensions of both the perceptual spaces, while Figure 8.6 shows the third and fourth dimension. The orientation of the axes in the MDS plot are irrelevant, so the plots for tool based interaction are rotated around for better visualization. Furthermore, the scaling of both the graphs was the same, therefore, they can be combined together without any scaling implications.

The perceptual space for the bare handed interaction in Figure 8.5 (see blue circles) show three very distinct clusters. The cloth-like surfaces are located in the left side of the graph, the rough surfaces take the top-center location while the right side of the graph consists of the smooth samples. The fact, that the clusters are very distinct and have relatively clear boundaries, means that it was easier to clearly distinguish the different texture surfaces.

On the other hand, the perceptual space for tool based interaction (Figure 8.5 see red circles) shows three clusters, but these groups are more diffused in nature. The nature of clusters is the same as bare handed perceptual space but the boundaries are not as clearly defined. This means

that the major texture categories were easily identifiable using both modes of interaction, but in the tool based interaction the minor differences in similar textures were also easily discriminable. This resulted in the diffused nature of the clusters.

Figure 8.6 shows the third and fourth dimension of both the modes of interaction. First we look at the bare handed perceptual space (see blue dots). The surfaces along the third dimension are very clearly scattered while the most of the samples along the fourth dimension are tightly clustered and do not show any visible trend. The third and fourth dimensions of the tool based perceptual (see red dots in Figure 8.6) space shows clear scattering of the surfaces. Despite the clear scattering, the surfaces seem to follow no trends at all. Unlike the first two dimensions, where the perceptual spaces showed similar characteristics, the third and fourth dimension for the two modes of interaction are quite different. This means that totally different classifying strategies were used by the participants along these dimensions.

8.2 Experiment - Adjective Rating

This experiment was conducted to evaluate the affective properties of the texture surfaces. The surfaces are rated against a set of adjective pairs to find out the adjectives which can define the properties of the surfaces. The details of this experiment are provided in the following subsection.

8.2.1 Participant and Stimuli

The six participants who took part in the perceptual space experiment were also part of this experiment. The experimental setup and conditions were the same as the first experiment.

Table 8.2: The list of adjectives used in the adjective rating experiment.

Sticky	Slippery	Flat	Even	Irritating
Rough	Hard	Dense	Bumpy	Pleasant
Sharp	Thick	Uneven	Dull	Sparse
Smooth	Prickly	Thin	Soothing	Soft

8.2.2   Procedure

The adjective rating experiment was divided into two parts. First, a list of adjectives was prepared which could describe the affective properties of all the surfaces used in the experiment. The participants were asked to feel all the surfaces and choose appropriate adjectives that could express the feeling of the surfaces. A list of 20 adjectives was provided, from which the participants had to chose the relevant adjectives. The list of these adjectives is given in Table 8.2.

The adjectives which were not selected by any participant were discarded. From the selected adjectives, adjective pairs were chosen in such a way that every adjective had a corresponding adjective with an opposite meaning. As a result of this procedure, we were left with five pairs of adjectives, which are shown in Table 8.3.

These five adjective pairs were used in the second part of the experiment. A Graphical User Interface (GUI) was built for conducting the experiment. There were sliders marked on the GUI having the adjective pairs at either end. The slider was not marked with any numbers and the total length of the slider on the screen was kept to 127 mm according to [94]. The values from the sliders were scaled from zero to 100. At the end, scores from all the participants were averaged.
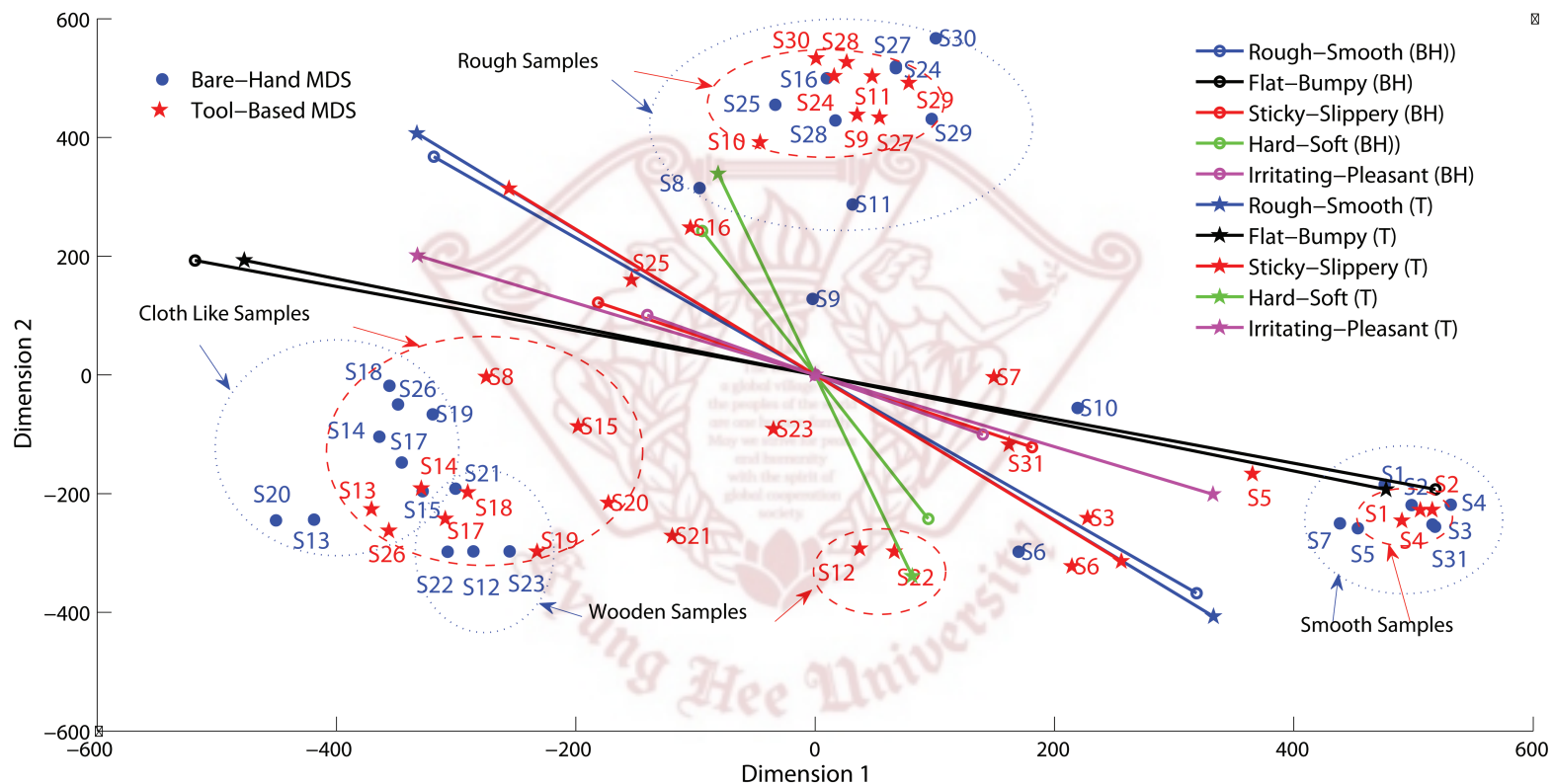
Figure 8.5: Dimensions one and two of the bare handed perceptual space established as a result of MDS analysis.
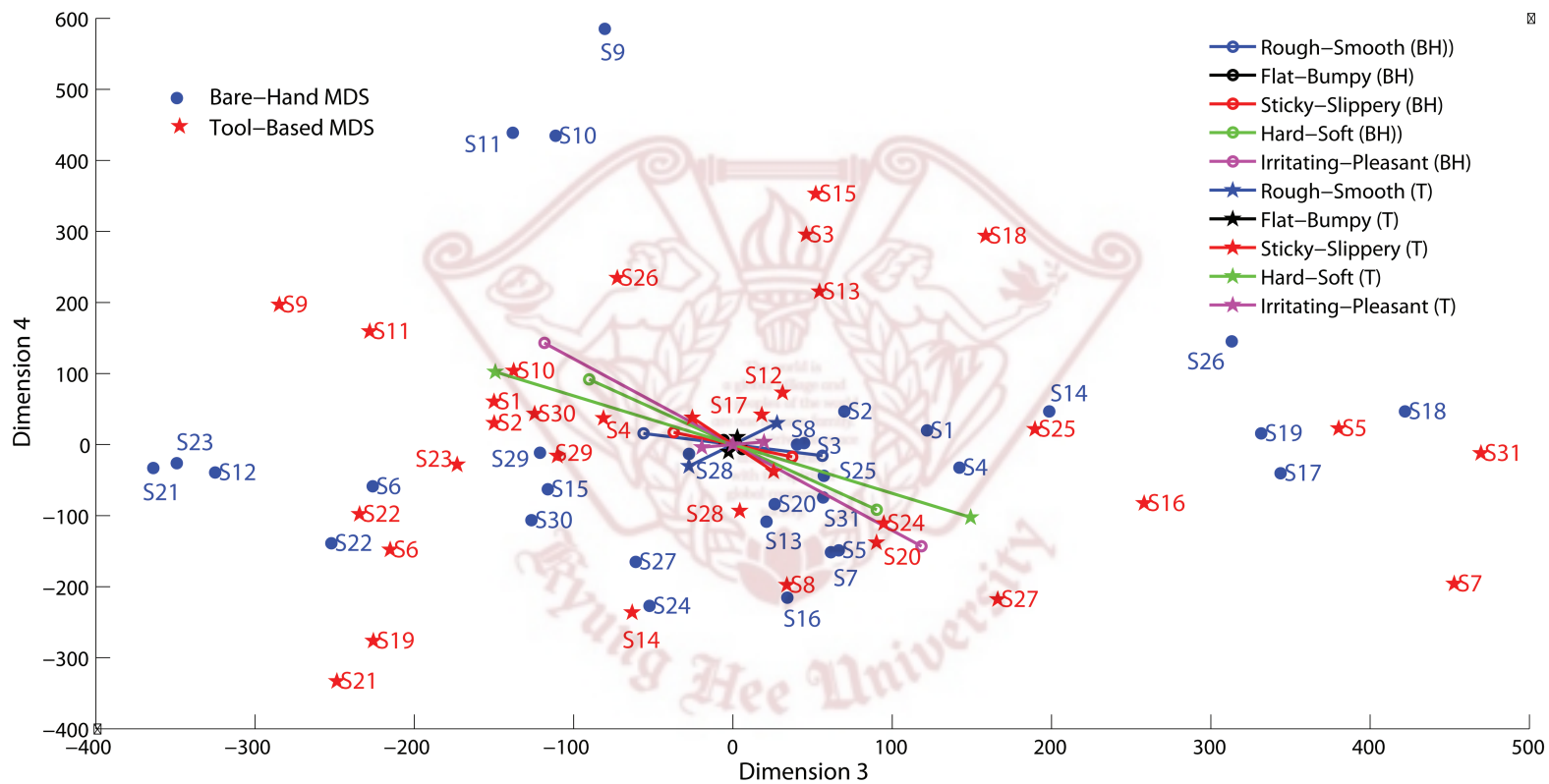
Figure 8.6: Dimensions three and four of the bare handed perceptual space established as a result of MDS analysis.

Table 8.3: List of adjective pairs after first part of the adjective rating experiment.

Adjective Pairs
Rough - Smooth
Flat - Bumpy
Sticky - Slippery
Hard - Soft
Irritating - Pleasant

8.2.3   Results

The adjective scores obtained from the adjective rating experiment provided us with the qualitative properties of the texture surfaces. To further validate the quality of these scores, correlation between the adjective scores and the perceptual space dimensions was calculated. The correlation values are shown in Table 8.4. It is evident that the correlation values of the adjective pairs Rough - Smooth and Flat - Bumpy for second dimension of both the perceptual spaces are quite high. It means that these two adjective pairs can account for a large portion of the variance along this dimension. Whereas, the correlations for the third and fourth dimension are quite low for most of the adjective pairs. This means that trends along these dimensions are not straightforward and the participants used totally other properties of the surface texture for classifying along these dimensions.

Multi-linear regression was performed to establish a relationship between the adjective pairs and the perceptual spaces. The inputs to the regression algorithm were the adjective scores and the Cartesian coordinates of the surfaces in the perceptual spaces. The linearly regressed lines in Figure 8.5 and Figure 8.6 show the adjective pairs. The length of the line is directly proportional to goodness of fit or the correlation between the associated

Table 8.4: Correlation between the five adjective pairs selected after the first part of adjective rating and the perceptual spaces for the bare handed and tool based interaction. The highlighted correlation values are considered as significant.

Adjective Pair	Tool Based			
Rough-Smooth	0.46	**-0.76**	0.12	-0.17
Flat-Bumpy	-0.48	**0.73**	0.03	-0.02
Sticky-Slippery	0.15	**-0.61**	-0.3	0.06
Hard-Soft	-0.49	-0.06	**0.57**	-0.25
Irritating-Pleasant	0.19	-0.74	-0.01	-0.02
	Bare Handed			
	Dim 1	**Dim 2**	**Dim 3**	**Dim 4**
Rough-Smooth	0.36	**-0.78**	0.13	-0.27
Flat-Bumpy	-0.27	**0.88**	-0.11	-0.01
Sticky-Slippery	0.04	**-0.58**	0.13	-0.21
Hard-Soft	**-0.57**	0.26	0.27	-0.35
Irritating-Pleasant	0.05	-0.51	0.33	-0.41

adjective pair and the perceptual space. Thus, a longer line means that the corresponding adjective pair can explain a large amount of variance along a specific dimension. The two adjective pairs which showed the highest correlation were Rough- Smooth and Flat - Bumpy. The adjective scores for these adjective pairs are provided in Figure 8.7 and Figure 8.8, respectively.

8.3 Discussion

The differences in the perceptual spaces for the two modes of interaction can be explained with the help of the differences in the adjective rating scores and some intuitive reasoning. Since the first two dimensions showed

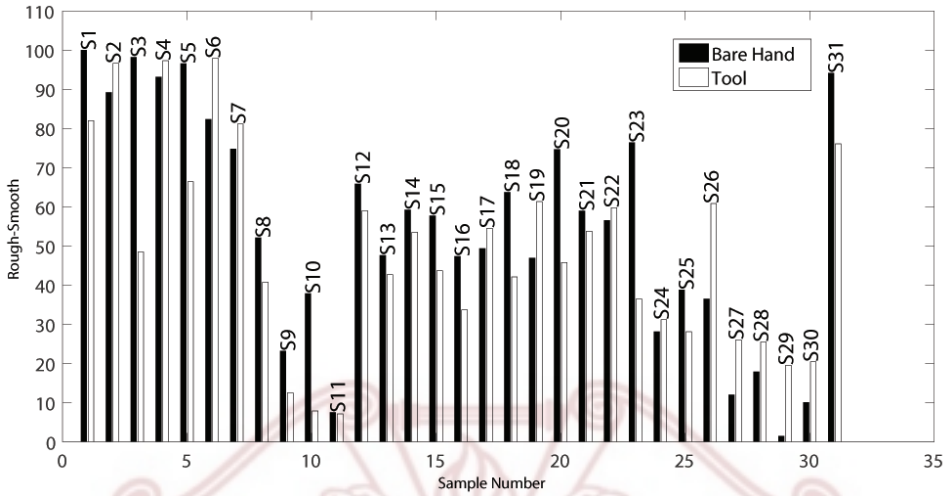**Figure 8.7:** The adjective scores obtained from the adjective rating experiment for the adjective pair of Rough - Smooth.
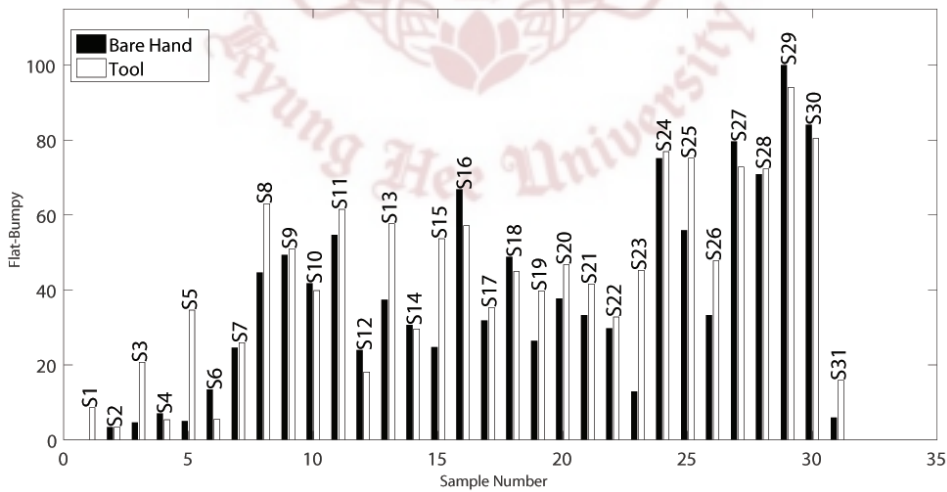

Figure 8.8: The adjective scores obtained from the adjective rating experiment for the adjective pair of Flat - Bumpy.

high correlation with the adjective pairs, this discussion will mostly focus on them.

8.3.1 Pre-Judgment in Classification Time

In our daily life mostly we use our bare hands for interacting with different surfaces. Due to familiarity, we can easily and quickly distinguish different surfaces. At the start of the experiment, the average classification time for one surface was around four to five seconds for both modes of interaction. But after some time, as the participants grew accustomed to the surfaces, the average time for bare handed interaction reduced to one or two seconds. Since, we can gather a lot more information when we interact through our hands, it became easy to judge surfaces immediately. In other words, the participants used pre-judgment in classifying the surfaces. Whereas, the classifying time for the tool based interaction almost remained constant throughout the experiment. This was due to the fact that the information passed on through a tool is very limited and it is difficult to get familiar with the surfaces. This also means that in the tool based interaction, the participants were using actual textural differences among the surfaces for classification, which made the classification more accurate. Thus it is safe to say that bare handed interaction has a higher classification speed while tool based interaction can provide better accuracy.

8.3.2 Pre-Judgment in Texture Evaluation

The above fact can be proved by an example from the perceptual space. The wooden surfaces form a typical example for pre-judgment, since it is fairly easy to identify a wooden surface using our hands. It was noticed that after a few trials as soon as a wooden sample was encountered by the participants during the bare handed interaction, it was immediately classified

into the group where other wooden surfaces were place. This classification occurred irrespective of the texture differences. The wooden surfaces S12, S21, S22, and S23 are located nearby each other in the perceptual space for bare handed interaction (see Figure 8.5). In tool based interaction, where the participants did not have direct contact with the surfaces, they used the actual surface texture for classification by differentiating the smoother wooden samples (S12, and S22) from the somewhat rougher woods (S21 and S23).

Another example of prejudgment can be found in the form of the smooth surfaces (S1 - S5). In the perceptual space for bare handed interaction, all the smooth surfaces were tightly packed together, whereas in tool based interaction the clustering was a little more diffused. This can be explained by the Rough- Smooth adjective rating scores of these surfaces for both modes of interaction. The bare hand adjective scores for all the smooth surfaces are almost similar, which means that participants did not cater for the texture differences. In tool based perceptual space, the very smooth surfaces (S1, S2, and S4) form a separate cluster from the other smooth surfaces (S3 and S5). This fact is also reflected in the adjective scores, i.e., S1, S2 and S4 have similar scores while S3 and S5 have lower scores.

8.3.3 The Masking Effect of Tool

When we interact with some object, the skin on our fingers gets deformed according to surface texture of that object. This deformation provides us cutaneous cues which help us in differentiating across textures. But in case of tool based interaction, this information is not available to us. Instead skin deformation occurs according to the shape of the tool. The only information available to the skin is through the vibrations of the tool. This effect was evident in the current comparison. The surfaces S16, a towel, and S8,

artificial grass, are near to the rough cluster in the bare handed perceptual space. Since these had quite rough texture, so they were correctly placed near the rougher surfaces. However, in the tool based perceptual space, these surfaces move away from the rough cluster. The roughness of these surfaces was soft in nature. The vibrations created by this roughness were not strong enough and due to the rigidity of the tool tip these vibrations were masked and never reached the skin of the participant. As a result they were perceived as smoother than they actually were.

8.3.4 Cross Modal Correlation Between Adjective Pairs

In the above discussion we mentioned some differences between the two modes of interaction. In order to check as to how much did these differences affect the perception across the two modes of interaction, we calculated the correlation between the adjective pairs for both modes of interaction. Table 8.5. The table shows that all the adjective pairs are very highly correlated, which means that similarities existed between the two modes of interaction, despite all the differences mentioned above.

Table 8.5: Correlation values between the adjective scores for bare handed and tool based interaction.

Adjective Pair	Correlation
Rough - Smooth	0.79
Flat - Bumpy	0.9
Sticky - Slippery	0.78
Hard- Soft	0.79
Irritating - Pleasant	0.84

8.4   Chapter Summary

In this chapter we provided an in-depth analysis of the perceptual differences between tool based and bare handed interaction. Various attributes associated with each mode of interaction were highlighted, which play a part in differentiating one from the other. Evidence of pre-judgment was found in bare handed interaction, while the masking effect in tool based interaction was also proved. The implications of pre-judgment were also discussed.

Chapter 9

Automatic Haptic Model Assignment to Mesh Objects

In Chapter 7, we evaluated the automatic assignment algorithm by using 21 new texture surfaces, where a model was assigned to the complete surface and it was assumed that the surface is uniform in texture, i.e., the surface contains just one texture. However, in real life scenarios certain surfaces may contain different surface textures. Moreover, most three dimensional haptic rendering interfaces work with mesh models, where (theoretically) every vertex is surrounded by a different texture. In such cases, we cannot directly assign a haptic model to the whole surface or object.

In order to handle this problem, the surface texture around each vertex was segmented and a unique haptic model was assigned to each of the segmented region.

As a proof of concept study, a cube was designed having a total of 152 vertices. Different textures were assigned to the faces of the cube. The surface texture was segmented into 152 parts (as we have 152 vertices), and each part was assigned a haptic model from the library.

9.1   3D Mesh Object

A three dimensional mesh object in the form a cube was designed using a graphics designing software, as shown in Figure 9.1. All the faces of the
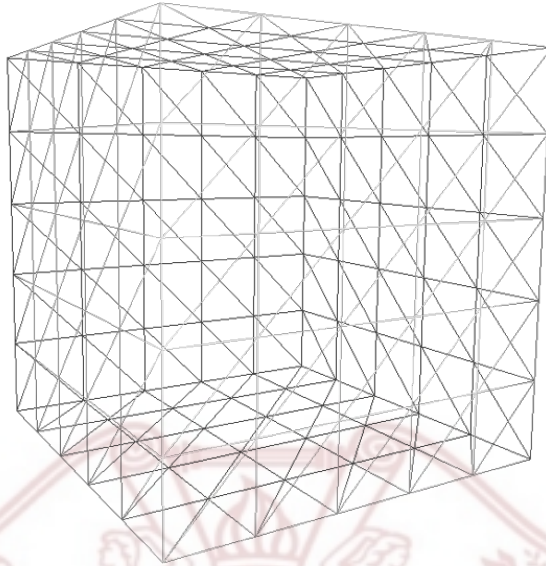
Figure 9.1: Mesh model of a cube having 152 vertices.

cube were wrapped with different textures. The surface texture image can be seen in Figure 9.2.

9.2   Vertex Based Automatic Assignment of Haptic Models to Mesh Object

In order to assign haptic models to the mesh, the surface texture around every vertex was extracted. The texture surrounding a specific vertex was considered for assigning a haptic model to the vertex. A window size of 300×300 pixels was cropped, having the associated vertex at the center. In this way a total of 152 sub-images were extracted from the wrapped texture image of the mesh model. A few of the sub-images can be seen in Figure 9.3. Each sub-image was assigned a haptic model based on its image features using the automatic assignment algorithm.
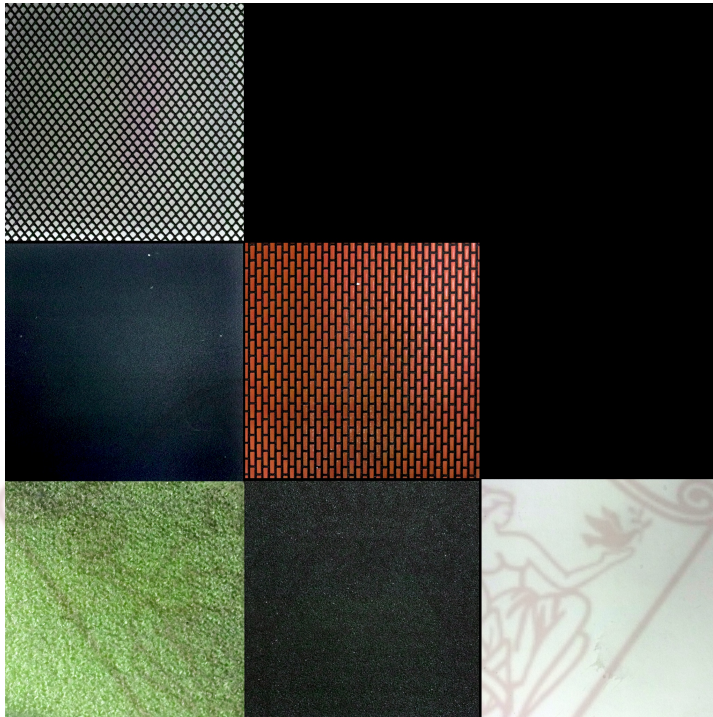
Figure 9.2: The surface textures used to wrap the six faces of the cube.
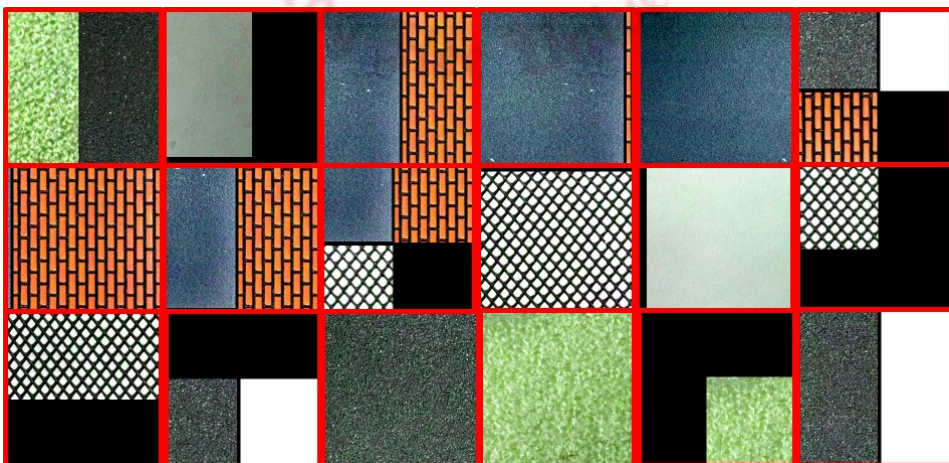
Figure 9.3: A few of the sub-images extracted from the texture image of the mesh model.

9.3   Chapter Summary

In this chapter we assigned haptic models to a mesh object in the form of
a cube. The assignment of haptic models was vertex based. The image
texture of the cube was segmented into smaller images surrounding all the
vertices. And the segmented images were used for assigning haptic models
to vertices using the automatic assignment algorithm.

Chapter 10
Conclusion and Future Work

This chapter provides a brief overview of the whole study. The significance and possible applications of the overall framework are also discussed here. Additionally, this chapter sheds some light on the possible future directions for this research.

10.1 Conclusion

The main goal of the current study was to built a universal haptic texture models library and use the library for automatic assignment of haptic texture models to various surfaces based on their image features. These goals were achieved by establishing a relationship between perceived haptic texture and image features of a given surface.

In order to built a library which can be used for assigning haptic texture models to any arbitrary surface, it should cover the major aspects of the daily life haptic interactions. For this purpose, a wide range of real life texture surfaces were used in building the library. Afterwards, the haptic perception information from these surfaces was captured by conducting a psychophysical experiment and consequently building a perceptual space. As a result of this experiment, a wide range of haptic perception information was stored in the perceptual space. The next step was to pictographically capture maximum haptic details of the texture surfaces used in building the

library. In order to capture the majority of the haptic details, a large number of image features were extracted from the surfaces. The perceptual space built from the psychophysical experiment and the image features extracted from the surfaces were combined in a relationship and this relationship was used for automatically associating haptic properties with newly encountered texture surfaces based on their image features.

The current study would go a long way in simplifying and standardizing the haptic modeling process. The current study eliminates the need to built a haptic model for every surface. Instead a perceptually similar haptic model can be readily assigned to a given surface.

Another dilemma in the current haptics research is that most of the haptic rendering systems employ tool based interaction while a majority of the psychophysical experiments are carried out using bare hands. The current study shed light on the differences between the two modes of interaction and highlighted that they differ in some aspects. However, the two modes of interaction operate quite similarly in a broad sense.

10.2   Future Work

A total of 84 different real life texture surfaces were used in the current study. Although, this a large number of surfaces having myriad surface textures, still there remains room for incorporating some totally different surfaces. For example, using oily or wet surfaces, organic surfaces, deformable surfaces etc. As a future direction, such surfaces can also be added to the library in addition to current ones.

In the current study it was assumed that the haptic models contained in the library are captured by data-driven modeling of the texture surfaces. As a possible avenue for further investigation can be the field of haptic
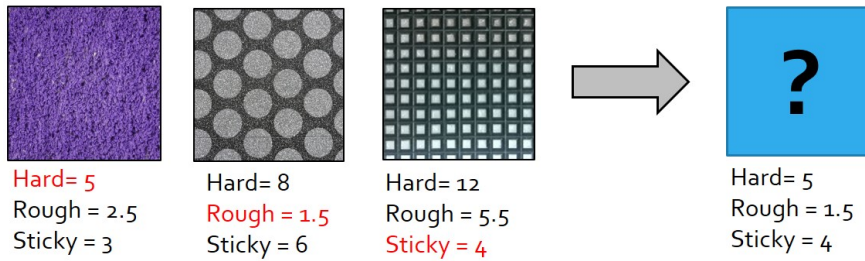
Figure 10.1: An example of haptic texture authoring.

texture authoring, where a haptic model is created from scratch instead of data driven modeling. The relationship between haptic texture and image features established in the current study can be generalized in this direction. This can be best explained with an example. Figure 10.1 shows three real life texture surfaces having well defined physical properties. The data driven models for these surfaces are also available. But our need is to render a new surface which can exhibit partial characteristics of the above mentioned three surfaces. This can be made possible only if we know the relationship between image features and the corresponding physical properties.

References

[1] Z. Merchant, E. T. Goetz, W. Keeney-Kennicutt, O.-m. Kwok, L. Cifuentes, and T. J. Davis, "The learner characteristics, features of desktop 3d virtual reality environments, and college chemistry instruction: A structural equation modeling analysis," *Computers & Education*, vol. 59, no. 2, pp. 551–568, 2012.

[2] Z. Merchant, E. T. Goetz, L. Cifuentes, W. Keeney-Kennicutt, and T. J. Davis, "Effectiveness of virtual reality-based instruction on students' learning outcomes in k-12 and higher education: A meta-analysis," *Computers & Education*, vol. 70, pp. 29–40, 2014.

[3] A. Pasqualotti and C. M. d. S. Freitas, "Mat3d: a virtual reality modeling language environment for the teaching and learning of mathematics," *CyberPsychology & Behavior*, vol. 5, no. 5, pp. 409–422, 2002.

[4] M. Kebritchi, A. Hirumi, and H. Bai, "The effects of modern mathematics computer games on mathematics achievement and class motivation," *Computers & education*, vol. 55, no. 2, pp. 427–443, 2010.

[5] S. Chan, F. Conti, K. Salisbury, and N. H. Blevins, "Virtual reality simulation in neurosurgery: technologies and evolution," *Neurosurgery*, vol. 72, pp. A154–A164, 2013.

[6] A. Renner, J. Holub, S. Sridhar, G. Evans, and E. Winer, "A virtual reality application for additive manufacturing process training," in *ASME 2015 International Design Engineering Technical Conferences and Computers and Information in Engineering Conference.* American Society of Mechanical Engineers, 2015, pp. V01AT02A033–V01AT02A033.

[7] G. Lorenzo, A. Lledó, J. Pomares, and R. Roig, "Design and application of an immersive virtual reality system to enhance emotional skills for children with autism spectrum disorders," *Computers & Education*, vol. 98, pp. 192–205, 2016.

[8] A. Miloff, P. Lindner, W. Hamilton, L. Reuterskiöld, G. Andersson, and P. Carlbring, "Single-session gamified virtual reality exposure therapy for spider phobia vs. traditional exposure therapy: study protocol for a randomized controlled non-inferiority trial," *Trials*, vol. 17, no. 1, p. 1, 2016.

[9] K. S. Hale and K. M. Stanney, *Handbook of virtual environments: Design, implementation, and applications.* CRC Press, 2014.

[10] O. Van der Meijden and M. Schijven, "The value of haptic feedback in conventional and robot-assisted minimal invasive surgery and virtual reality training: a current review," *Surgical endoscopy*, vol. 23, no. 6, pp. 1180–1190, 2009.

[11] C. Colwell, H. Petrie, D. Kornbrot, A. Hardwick, and S. Furner, "Haptic virtual reality for blind computer users," in *Proceedings of the third international ACM conference on Assistive technologies.* ACM, 1998, pp. 92–99.

[12] G. M. Lemole Jr, P. P. Banerjee, C. Luciano, S. Neckrysh, and F. T. Charbel, "Virtual reality in neurosurgical education: Part-task ventriculostomy simulation with dynamic visual and haptic feedback," *Neurosurgery*, vol. 61, no. 1, pp. 142–149, 2007.

[13] M. Azmandian, M. Hancock, H. Benko, E. Ofek, and A. D. Wilson, "A demonstration of haptic retargeting: Dynamic repurposing of passive haptics for enhanced virtual reality experience," in *Proceedings of the 2016 CHI Conference Extended Abstracts on Human Factors in Computing Systems.* ACM, 2016, pp. 3647–3650.

[14] D. C. Ruspini, K. Kolarov, and O. Khatib, "The haptic display of complex graphical environments," in *Proceedings of the 24th annual conference on Computer graphics and interactive techniques.* ACM Press/Addison-Wesley Publishing Co., 1997, pp. 345–352.

[15] S. Jeon and S. Choi, "Real stiffness augmentation for haptic augmented reality," *Presence: Teleoperators and Virtual Environments*, vol. 20, no. 4, pp. 337–370, 2011.

[16] T. Yamamoto, B. Vagvolgyi, K. Balaji, L. L. Whitcomb, and A. M. Okamura, "Tissue property estimation and graphical display for teleoperated robot-assisted surgery," in *Robotics and Automation, 2009. ICRA'09. IEEE International Conference on.* IEEE, 2009, pp. 4239–4245.

[17] A. M. Okamura, M. R. Cutkosky, and J. T. Dennerlein, "Reality-based models for vibration feedback in virtual environments," *Mechatronics, IEEE/ASME Transactions on*, vol. 6, no. 3, pp. 245–252, 2001.

[18] R. Hover, G. Kósa, G. Székely, and M. Harders, "Data-driven haptic rendering?from viscous fluids to visco-elastic solids," *Haptics, IEEE Transactions on*, vol. 2, no. 1, pp. 15–27, 2009.

[19] M. Mahvash and V. Hayward, "High-fidelity haptic synthesis of contact with deformable bodies," *Computer Graphics and Applications, IEEE*, vol. 24, no. 2, pp. 48–55, 2004.

[20] P. Fong, "Sensing, acquisition, and interactive playback of data-based models for elastic deformable objects," *The International Journal of Robotics Research*, vol. 28, no. 5, pp. 630–655, 2009.

[21] K. E. MacLean, "The haptic camera: A technique for characterizing and playing back haptic properties of real environments," *Proc. of Haptic Interfaces for Virtual Environments and Teleoperator Systems (HAPTICS)*, pp. 459–467, 1996.

[22] L. Kim, G. S. Sukhatme, and M. Desbrun, "Haptic editing of decoration and material properties," in *Haptic Interfaces for Virtual Environment and Teleoperator Systems, 2003. HAPTICS 2003. Proceedings. 11th Symposium on*. IEEE, 2003, pp. 213–220.

[23] D. Katz, "The world of touch (le krueger, trans.)," *Mahwah. NJ: Rrlbaum.(Original work published 1925)*, 1989.

[24] M. YOSHIDA, "Dimensions of tactual impressions (1)," *Japanese Psychological Research*, vol. 10, no. 3, pp. 123–137, 1968.

[25] M. Hollins, S. Bensmaïa, K. Karlof, and F. Young, "Individual differences in perceptual space for tactile textures: Evidence from multidimensional scaling," *Perception & Psychophysics*, vol. 62, no. 8, pp. 1534–1544, 2000.

[26] S. Okamoto, H. Nagano, and Y. Yamada, "Psychophysical dimensions of tactile perception of textures," *Haptics, IEEE Transactions on*, vol. 6, no. 1, pp. 81–93, 2013.

[27] R. H. LaMotte, "Softness discrimination with a tool," *Journal of Neurophysiology*, vol. 83, no. 4, pp. 1777–1786, 2000.

[28] M. Hollins, F. Lorenz, A. Seeger, and R. Taylor, "Factors contributing to the integration of textural qualities: Evidence from virtual surfaces," *Somatosensory & motor research*, vol. 22, no. 3, pp. 193–206, 2005.

[29] R. Klatzky, S. Lederman, C. Hamilton, and G. Ramsay, "Perceiving roughness via a rigid probe: Effects of exploration speed," in *Proceedings of the ASME Dynamic Systems and Control Division*, vol. 67, 1999, pp. 27–33.

[30] T. Yoshioka, S. Bensmaia, J. Craig, and S. Hsiao, "Texture perception through direct and indirect touch: An analysis of perceptual space for tactile textures in two modes of exploration," *Somatosensory & motor research*, vol. 24, no. 1-2, pp. 53–70, 2007.

[31] W. Hassan and S. Jeon, "Evaluating differences between bare-handed and tool-based interaction in perceptual space," in *2016 IEEE Haptics Symposium (HAPTICS)*.   IEEE, 2016, pp. 185–191.

[32] J. Wu, A. Song, and C. Zou, "A novel haptic texture display based on image processing," in *Robotics and Biomimetics, 2007. ROBIO 2007. IEEE International Conference on*.   IEEE, 2007, pp. 1315–1320.

[33] T. Ping-Sing and M. Shah, "Shape from shading using linear approximation," *Image and Vision computing*, vol. 12, no. 8, pp. 487–498, 1994.

[34] R. Zhang, P. Tsai, J. Cryer, and M. Shah, "Shape-fromshading: a survey. pattern analysis and machine intelligence," *IEEE Transactions on*, vol. 21, no. 8, pp. 690–706, 1999.

[35] H. Culbertson, J. Unwin, and K. J. Kuchenbecker, "Modeling and rendering realistic textures from unconstrained tool-surface interactions," *Haptics, IEEE Transactions on*, vol. 7, no. 3, pp. 381–393, 2014.

[36] L. A. Jones and S. J. Lederman, *Human hand function.* Oxford University Press, 2006.

[37] S. J. Lederman and R. L. Klatzky, "Haptic perception: A tutorial," *Attention, Perception, & Psychophysics*, vol. 71, no. 7, pp. 1439–1459, 2009.

[38] W. M. B. Tiest, "Tactual perception of material properties," *Vision research*, vol. 50, no. 24, pp. 2775–2782, 2010.

[39] D. Picard, C. Dacremont, D. Valentin, and A. Giboreau, "About the salient perceptual dimensions of tactile texture space," *Touch, Blindness and Neuroscience Eds S Ballesteros, M Heller*, pp. 165–174, 2004.

[40] I. Soufflet, M. Calonnier, and C. Dacremont, "A comparison between industrial experts' and novices' haptic perceptual organization: A tool to identify descriptors of the handle of fabrics," *Food quality and preference*, vol. 15, no. 7, pp. 689–699, 2004.

[41] M. Lyne, A. Whiteman, and D. Donderi, "Multidimensional scaling of tissue quality," *Pulp & Paper Canada*, vol. 85, no. 10, pp. 43–50, 1984.

[42] M. Holliins, R. Faldowski, S. Rao, and F. Young, "Perceptual dimensions of tactile surface texture: A multidimensional scaling analysis," *Perception & psychophysics*, vol. 54, no. 6, pp. 697–705, 1993.

[43] S. Ballesteros, J. M. Reales, L. P. De León, and B. García, "The perception of ecological textures by touch: does the perceptual space change under bimodal visual and haptic exploration?" in *Eurohaptics Conference, 2005 and Symposium on Haptic Interfaces for Virtual Environment and Teleoperator Systems, 2005. World Haptics 2005. First Joint.* IEEE, 2005, pp. 635–638.

[44] W. M. B. Tiest and A. M. Kappers, "Analysis of haptic perception of materials by multidimensional scaling and physical measurements of roughness and compressibility," *Acta psychologica*, vol. 121, no. 1, pp. 1–20, 2006.

[45] C. E. Osgood and G. J. Suci, "Ph tannenbaum the measurement of meaning," *University of Illinois Press*, vol. 6, pp. 1880–1886, 1957.

[46] H. Shirado and T. Maeno, "Modeling of human texture perception for tactile displays and sensors," in *null.* IEEE, 2005, pp. 629–630.

[47] A. Giboreau, S. Navarro, P. Faye, and J. Dumortier, "Sensory evaluation of automotive fabrics: the contribution of categorization tasks and non verbal information to set-up a descriptive method of tactile properties," *Food quality and preference*, vol. 12, no. 5, pp. 311–322, 2001.

[48] J. Pasquero, J. Luk, S. Little, and K. MacLean, "Perceptual analysis of haptic icons: an investigation into the validity of cluster sorted mds," in *Haptic Interfaces for Virtual Environment and Teleoperator Systems, 2006 14th Symposium on.* IEEE, 2006, pp. 437–444.

[49] F. Wickelmaier, "An introduction to mds," *Sound Quality Research Unit, Aalborg University, Denmark*, p. 46, 2003.

[50] R. A. Rao and G. L. Lohse, "Towards a texture naming system: identifying relevant dimensions of texture," in *Visualization, 1993. Visualization'93, Proceedings., IEEE Conference on.* IEEE, 1993, pp. 220–227.

[51] R. M. Haralick, K. Shanmugam, and I. H. Dinstein, "Textural features for image classification," *Systems, Man and Cybernetics, IEEE Transactions on*, no. 6, pp. 610–621, 1973.

[52] L.-K. Soh and C. Tsatsoulis, "Texture analysis of sar sea ice imagery using gray level co-occurrence matrices," *Geoscience and Remote Sensing, IEEE Transactions on*, vol. 37, no. 2, pp. 780–795, 1999.

[53] D. A. Clausi, "An analysis of co-occurrence texture statistics as a function of grey level quantization," *Canadian Journal of remote sensing*, vol. 28, no. 1, pp. 45–62, 2002.

[54] B. Julesz, "Visual pattern discrimination," *Information Theory, IRE Transactions on*, vol. 8, no. 2, pp. 84–92, 1962.

[55] B. Julesz, E. Gilbert, L. Shepp, and H. Frisch, "Inability of humans to discriminate between visual textures that agree in second-order statistics?revisited," *Perception*, vol. 2, no. 4, pp. 391–405, 1973.

[56] M. Amadasun and R. King, "Textural features corresponding to textural properties," *Systems, Man and Cybernetics, IEEE Transactions on*, vol. 19, no. 5, pp. 1264–1274, 1989.

[57] M. M. Galloway, "Texture analysis using gray level run lengths," *Computer graphics and image processing*, vol. 4, no. 2, pp. 172–179, 1975.

[58] A. Chu, C. M. Sehgal, and J. F. Greenleaf, "Use of gray value distribution of run lengths for texture analysis," *Pattern Recognition Letters*, vol. 11, no. 6, pp. 415–419, 1990.

[59] B. V. Dasarathy and E. B. Holder, "Image characterizations based on joint gray level-run length distributions," *Pattern Recognition Letters*, vol. 12, no. 8, pp. 497–502, 1991.

[60] G. Thibault, B. Fertil, C. Navarro, S. Pereira, P. Cau, N. Levy, J. Sequeira, and J. Mari, "Texture indexes and gray level size zone matrix application to cell nuclei classification," 2009.

[61] G. Elkharraz, S. Thumfart, D. Akay, C. Eitzinger, and B. Henson, "Making tactile textures with predefined affective properties," *Affective Computing, IEEE Transactions on*, vol. 5, no. 1, pp. 57–70, 2014.

[62] J. Kannala and E. Rahtu, "Bsif: Binarized statistical image features," in *Pattern Recognition (ICPR), 2012 21st International Conference on*. IEEE, 2012, pp. 1363–1366.

[63] D. Picard, C. Dacremont, D. Valentin, and A. Giboreau, "Perceptual dimensions of tactile textures," *Acta psychologica*, vol. 114, no. 2, pp. 165–184, 2003.

[64] I. R. Summers, R. J. Irwin, and A. C. Brady, "Haptic discrimination of paper," in *Human Haptic Perception: Basics and Applications*. Springer, 2008, pp. 525–535.

[65] J. B. Kruskal, "Multidimensional scaling by optimizing goodness of fit to a nonmetric hypothesis," *Psychometrika*, vol. 29, no. 1, pp. 1–27, 1964.

[66] B. S. Manjunath and W.-Y. Ma, "Texture features for browsing and retrieval of image data," *Pattern Analysis and Machine Intelligence, IEEE Transactions on*, vol. 18, no. 8, pp. 837–842, 1996.

[67] A. Oonsivilai and N. Meeboon, "Silk texture defect recognition system using computer vision and artificial neural networks," in *Image and Signal Processing, 2009. CISP'09. 2nd International Congress on.* IEEE, 2009, pp. 1–4.

[68] B. Lee and Y. Tarng, "Surface roughness inspection by computer vision in turning operations," *International Journal of Machine Tools and Manufacture*, vol. 41, no. 9, pp. 1251–1263, 2001.

[69] S.-Y. Ho, K.-C. Lee, S.-S. Chen, and S.-J. Ho, "Accurate modeling and prediction of surface roughness by computer vision in turning operations using an adaptive neuro-fuzzy inference system," *International Journal of Machine Tools and Manufacture*, vol. 42, no. 13, pp. 1441–1446, 2002.

[70] T. Özel and Y. Karpat, "Predictive modeling of surface roughness and tool wear in hard turning using regression and neural networks," *International Journal of Machine Tools and Manufacture*, vol. 45, no. 4, pp. 467–479, 2005.

[71] A. M. Deris, A. M. Zain, and R. Sallehuddin, "Hybrid gr-svm for prediction of surface roughness in abrasive water jet machining," *Meccanica*, vol. 48, no. 8, pp. 1937–1945, 2013.

[72] A. W. Whitney, "A direct method of nonparametric measurement selection," *Computers, IEEE Transactions on*, vol. 100, no. 9, pp. 1100–1103, 1971.

[73] R. Kohavi and G. H. John, "Wrappers for feature subset selection," *Artificial intelligence*, vol. 97, no. 1, pp. 273–324, 1997.

[74] B. Thompson and L. G. Daniel, "Factor an alytic evidence for the construct validity of scores: A historical overview and some guidelines,"

Educational and psychological measurement, vol. 56, no. 2, pp. 197–208, 1996.

[75] J. C. Hayton, D. G. Allen, and V. Scarpello, "Factor retention decisions in exploratory factor analysis: A tutorial on parallel analysis," *Organizational research methods*, vol. 7, no. 2, pp. 191–205, 2004.

[76] R. M. Haralock and L. G. Shapiro, *Computer and Robot Vision*, 1st ed. Boston, MA, USA: Addison-Wesley Longman Publishing Co., Inc., 1991.

[77] E. Langford, "Quartiles in elementary statistics." *Journal of Statistics Education*, vol. 14, no. 3, p. n3, 2006.

[78] C. Eaton, W. Velicer, and J. Fava, "Determining the number of components: An evaluation of parallel analysis and the minimum average partial correlation procedures," *Unpublished manuscript*, 1999.

[79] W. F. Velicer, C. A. Eaton, and J. L. Fava, "Construct explication through factor or component analysis: A review and evaluation of alternative procedures for determining the number of factors or components," in *Problems and solutions in human assessment*. Springer, 2000, pp. 41–71.

[80] L. W. Glorfeld, "An improvement on horn's parallel analysis methodology for selecting the correct number of factors to retain," *Educational and psychological measurement*, vol. 55, no. 3, pp. 377–393, 1995.

[81] R. G. Montanelli Jr and L. G. Humphreys, "Latent roots of random data correlation matrices with squared multiple correlations on the diagonal: A monte carlo study," *Psychometrika*, vol. 41, no. 3, pp. 341–348, 1976.

[82] N. E. Turner, "The effect of common variance and structure pattern on random data eigenvalues: Implications for the accuracy of parallel analysis," *Educational and Psychological Measurement*, vol. 58, no. 4, pp. 541–568, 1998.

[83] J. Weston and C. Watkins, "Multi-class support vector machines," Citeseer, Tech. Rep., 1998.

[84] C. Cortes and V. Vapnik, "Support-vector networks," *Machine learning*, vol. 20, no. 3, pp. 273–297, 1995.

[85] V. Vapnik, *The nature of statistical learning theory*. Springer Science & Business Media, 2013.

[86] V. N. Vapnik and V. Vapnik, *Statistical learning theory*. Wiley New York, 1998, vol. 1.

[87] G. Orrù, W. Pettersson-Yeo, A. F. Marquand, G. Sartori, and A. Mechelli, "Using support vector machine to identify imaging biomarkers of neurological and psychiatric disease: a critical review," *Neuroscience & Biobehavioral Reviews*, vol. 36, no. 4, pp. 1140–1152, 2012.

[88] C.-W. Hsu and C.-J. Lin, "A comparison of methods for multiclass support vector machines," *Neural Networks, IEEE Transactions on*, vol. 13, no. 2, pp. 415–425, 2002.

[89] B. SchiilkopP, C. Burgest, and V. Vapnik, "Extracting support data for a given task," *no. x*, 1995.

[90] I. Tsochantaridis, T. Hofmann, T. Joachims, and Y. Altun, "Support vector machine learning for interdependent and structured output

spaces," in *Proceedings of the twenty-first international conference on Machine learning.* ACM, 2004, p. 104.

[91] P. Janik and T. Lobos, "Automated classification of power-quality disturbances using svm and rbf networks," *Power Delivery, IEEE Transactions on*, vol. 21, no. 3, pp. 1663–1669, 2006.

[92] P. Chatterjee and N. R. Pal, "Discovery of synergistic genetic network: a minimum spanning tree-based approach," *Journal of bioinformatics and computational biology*, p. 1650003, 2015.

[93] D. Arthur and S. Vassilvitskii, "k-means++: The advantages of careful seeding," in *Proceedings of the eighteenth annual ACM-SIAM symposium on Discrete algorithms.* Society for Industrial and Applied Mathematics, 2007, pp. 1027–1035.

[94] I. Hwang and S. Choi, "Perceptual space and adjective rating of sinusoidal vibrations perceived via mobile device," in *Haptics Symposium, 2010 IEEE.* IEEE, 2010, pp. 1–8.

Appendix A

List of Publications

Haptics

1. [Conference Publication]: **Waseem Hassan**, and Seokhee Jeon, "Evaluating Differences Between Bare-Handed and Tool-based Interaction in Perceptual Space", 2016 IEEE Haptics Symposium (HAPTICS). IEEE, 2016.

2. [Conference Publication]: Noman Akbar, **Waseem Hassan**, Arsen Abdulali, and Seokhee Jeon, "Towards Automatic Haptic Texture Authoring Based on Image Texture Feature", in Proceedings of Korea Computer Congress, pp.1398-1400, 2015.

3. [Journal Publication]: Arsen Abdulai, **Waseem Hassan**, and Seokhee Jeon, "Stimuli-Magnitude-Adaptive Sample Selection for Data-Driven Haptic Modeling", Entropy 18.6 (2016): 222. **Impact Factor : 1.743**.

4. [Conference Publication]: **Waseem Hassan**, and Seokhee Jeon, "Building Haptic Texture Perceptual Space From Real-Life Textured Surfaces Using Multidimensional Scaling", in Proceedings of Korea Computer Congress, 2016. **(Accepted)**

5. [Journal Publication]: **Waseem Hassan**, Arsen Abdulai, and Seokhee Jeon, "Towards Universal Haptic Library Library-Based

Haptic Texture Selection Using Image Texture", IEEE Transactions on Haptics, **(Submission Ready)**

International Conference: Nonreferred Papers/

Posters/Demonstrations

6. [Conference Publication]: **Waseem Hassan**, and Seokhee Jeon, "Towards Universal Haptic Library Library-Based Haptic Texture Selection Using Image Texture", WIP, Eurohaptics. 2016. **(Accepted)**

7. [Conference Publication]: **Waseem Hassan**, Arsen Abdulai, and Seokhee Jeon, "Towards Universal Haptic Library Library-Based Haptic Texture Selection Using Image Texture", Demonstration, Eurohaptics. 2016. **(Accepted)**

Other Collaborative Work

8. [Journal Publication]: Idris, Muhammad, **Waseem Hassan**, Shujaat Hussain, Muhammad Hameed Siddiqi, Hafiz Syed Muhammad Bilal, and Sungyoung Lee. "MRPack: Multi-Algorithm Execution Using Compute-Intensive Approach in MapReduce." PloS one 10, no. 8 (2015): e0136259 **Impact Factor : 3.234**.